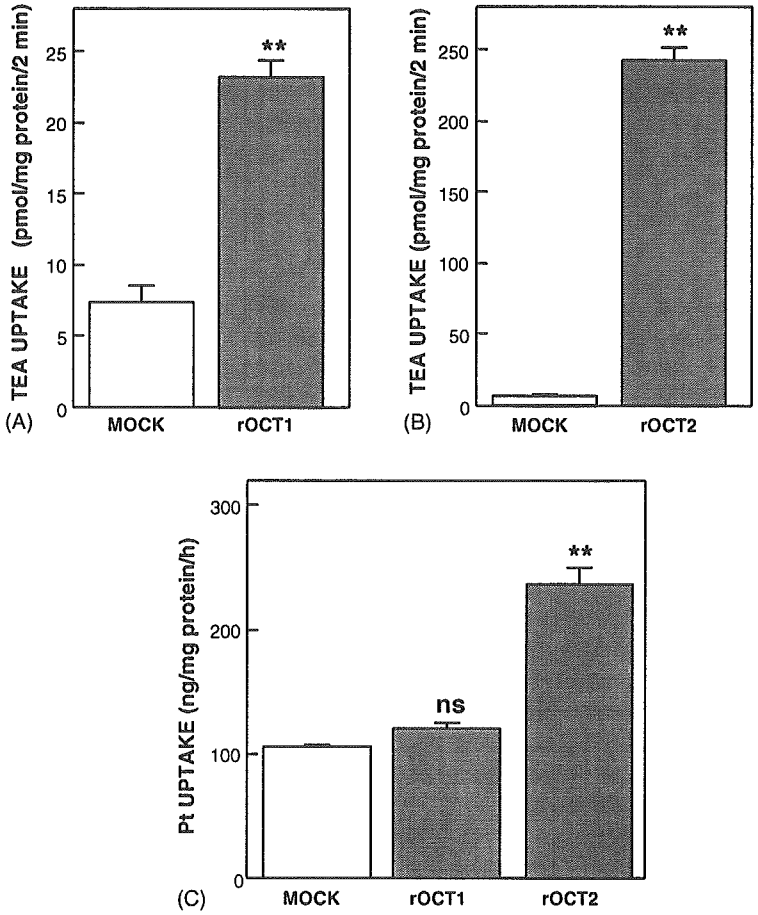

Fig. 3. rOCT1 or rOCT2-mediated uptake of cisplatin. HEK293 cells transiently expressing pBK-CMV (MOCK), rOCT1 or rOCT2 were incubated with 50 μM [^{14}C]TEA for 2 min (A and B) or 500 μM cisplatin for 1 h (C). The amount of [^{14}C]TEA or platinum was determined. Each point represents the mean ± S.E.M. of three or four wells. ns, not significantly; $^{**}P < 0.01$, significantly different from MOCK cells.

respectively (Fig. 2A). After the incubation with 500 μM cisplatin for 1 h, the amounts of platinum in HEK-pBK cells and HEK-rOCT2 cells were 90.0 ± 2.8 and 447.7 ± 5.3 ng/mg protein/h, respectively (Fig. 2B). Moreover, the accumulation of platinum by HEK-rOCT2 cells was inhibited in the presence of 1 mM cimetidine or 100 μM corticosterone (Fig. 2C).

3.4. Transport of cisplatin by HEK293 cells transiently expressing rOCT1 and rOCT2

Following the transfection of rOCT1 or rOCT2 cDNA, the mRNA expression levels of these transporters were 8037 ± 701 and 5834 ± 306 amol/mg protein (mean ± S.E.M. of four monolayers), respectively. Uptake of [^{14}C]TEA was observed in HEK293 cells transiently expressing rOCT1 or rOCT2 (Fig. 3A and B). However, the amount of platinum accumulated in the HEK293 cells transiently transfected with pBK-CMV, rOCT1 and rOCT2 was 107.8 ± 1.1, 122.4 ± 4.0 (ns versus pBK-CMV) and 237.6 ± 13.8 ($P < 0.01$ versus pBK-CMV) ng/mg protein/h, respectively (Fig. 3C).

3.5. Pharmacokinetics of cisplatin in male and female rats

We compared the pharmacokinetics of cisplatin between male and female rats, because it was found that the expression level of renal rOCT2, but not rOCT1, was much higher in male rats than female rats [18]. The plasma concentrations of platinum up to 3 min after the administration of cisplatin as a bolus were determined (Fig. 4A). The total clearance (CL_{total}) of cisplatin, which was calculated from the dose and area under the concentration-time curve (AUC) of cisplatin for 3 min, was 35.1 ± 3.5 ml/min and 16.8 ± 1.1 ml/min in male and female rats, respectively (Fig. 4B). The tissue uptake clearance (CL_{tissue}), which was calculated from the AUC of cisplatin for 3 min and the amount of cisplatin in tissue at 3 min, was also examined. The renal CL_{tissue} was significantly greater in male rats (13.2 ± 1.3 ml/min) than female rats (5.9 ± 0.4 ml/min). However, hepatic CL_{tissue} in male rats (3.7 ± 0.3 ml/min) was not significantly different from that in female rats (2.6 ± 0.2 ml/min) (Fig. 4C). In addition, the male-dominant expression of

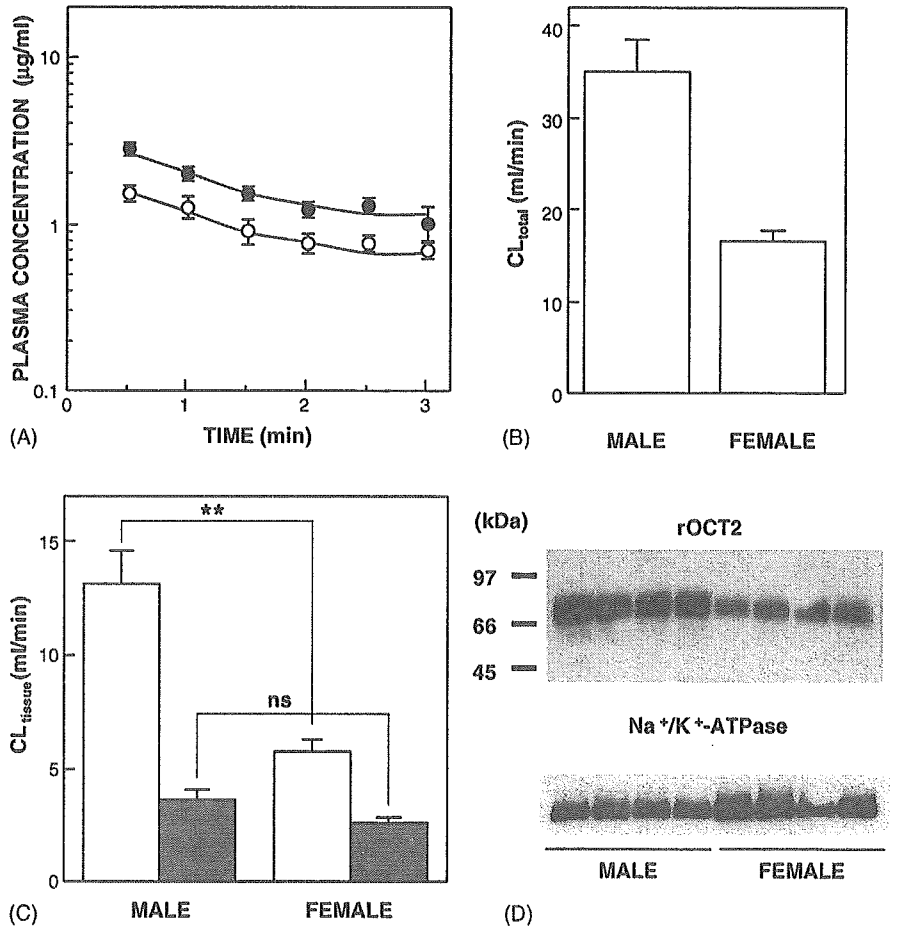

Fig. 4. Pharmacokinetics of cisplatin in male and female rats. (A) Plasma concentrations of platinum at various points were determined in male (open circle) and female (closed circle) rats. Total clearance (CL_{total}; B) and tissue uptake clearance (CL_{tissue}; C: renal CL_{tissue} (open column) and hepatic CL_{tissue} (closed column)) were calculated by dividing the administered dose or the amount in tissue at 3 min by the area under the curve (AUC) from 0 to 3 min, respectively. Each column represents the mean ± S.E.M. of five rats. ns, not significantly different; $^{**}P < 0.01$, significantly different. (D) Protein expression of rOCT2 and Na^+/K^+-ATPase in male and female rats. Representative photographs of Western blotting are shown.

the renal rOCT2 was confirmed by Western blotting (Fig. 4D).

3.6. Renal functional data of male rats treated with cisplatin

The male rats showed renal tubular toxicity 2 days after the administration of 2 mg/kg of cisplatin. The body weight, plasma creatinine level, creatinine clearance, blood urea nitrogen (BUN), urinary albumin level, aspartate aminotransferase (AST), alanine aminotransferase (ALT) and total bilirubin level were unaffected. However, *N*-acetyl-β-D-glucosaminidase (NAG) activity and urine volume were significantly increased in the male rats treated with cisplatin compared to the control rats (Table 1).

To confirm the contribution of renal rOCT2 expression on cisplatin-induced tubulotoxicity, we compared the NAG

Table 1
Biochemical parameters in male rats treated with cisplatin (2 mg/kg)

	Sham	Cisplatin
Body weight (g)	281 ± 4	274 ± 3
Urine volume (ml/24 h)	10.9 ± 0.9	22.4 ± 2.9**
NAG (U/day)	129 ± 42	317 ± 47**
Pcre (mg/dl)	0.42 ± 0.02	0.50 ± 0.03
Ccr (ml/min/kg)	5.81 ± 0.08	5.96 ± 0.06
BUN (mg/dl)	14.9 ± 0.3	14.2 ± 0.6
Urinary albumin (mg/day)	0.24 ± 0.06	0.44 ± 0.08
AST (IU/l)	61.8 ± 4.0	76.1 ± 6.2
ALT (IU/l)	15.0 ± 1.3	18.8 ± 1.7
T-Bil (mg/dl)	0.05 ± 0.01	0.11 ± 0.04

Values represent means ± S.E.M. of nine rats. NAG, *N*-acetyl-β-D-glucosaminidase; Pcre, plasma creatinine; Ccr, creatinine clearance; BUN, blood urea nitrogen; AST, aspartate aminotransferase; ALT, alanine aminotransferase; T-Bil, total bilirubin.
** $P < 0.01$, significantly different from sham.

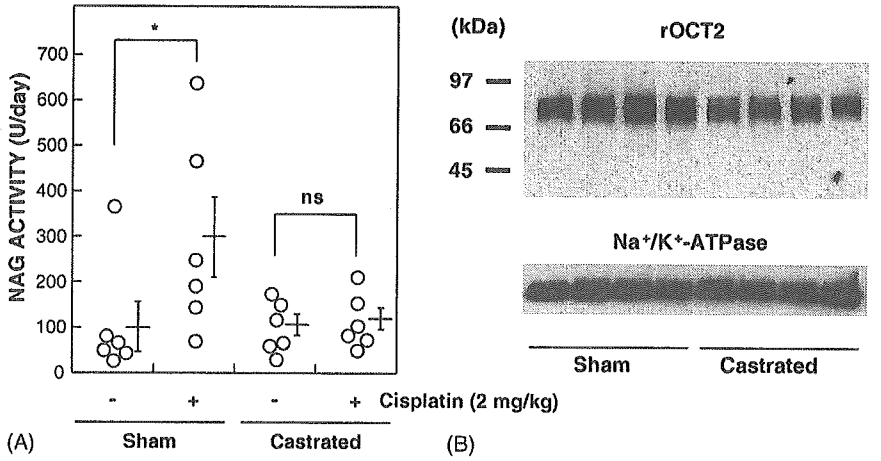

Fig. 5. Effect of the castration on cisplatin-induced tubular toxicity and renal rOCT2 expression. Male rats (5 weeks) were surgically castrated, and fed and given water freely for 3 weeks. (A) The NAG activity in bladder urine in the sham-operated or castrated rats 2 days after the administration of 2 mg/mg of cisplatin ($n = 6$). Each bar represents the mean ± S.E.M. of six rats. ns, not significantly different; $^{*}P < 0.05$, significantly different. (B) Protein expression of rOCT2 and Na^{+}/K^{+}-ATPase in the sham-operated or castrated rats. Representative photographs of Western blotting are shown.

activity in bladder urine between the sham-operated and castrated male rats. The serum concentrations of testosterone were 1.56 ± 0.11 and 0.25 ± 0.04 ng/ml (mean ± S.E.M. of 12 rats; $P < 0.01$) in the sham-operated and castrated rats, respectively. Two days after the administration of 2 mg/kg of cisplatin, NAG activity was significantly increased in the sham-operated rats. On the other hand, 2 mg/kg of cisplatin was not enough to increase urinary NAG activity in the castrated rats (Fig. 5A). The renal rOCT2 expression was decreased in the castrated rats compared to the sham-operated rats (Fig. 5B).

4. Discussion

Using cultured renal epithelial cells, cisplatin was found to be accumulated from the basolateral membranes via a specific carrier system [6,7,20]. In OK cells, the basolateral uptake of cisplatin was decreased in the presence of TEA [20]. Ludwig et al. [7] reported that cisplatin-induced cytotoxicity was ameliorated in the presence of cimetidine in MDCK-C7 cells. Although a polyclonal antibody against rat OCT2 (OCT2-A®, Alpha-diagnostic, San Antonio, TX) showed two signals, 65 and 50 kDa [7], the amino acid sequence of the antigen peptide was conserved 76% in mouse, 66% in porcine and 57% in human (http://www.4adi.com/data/oat/oct21.html). Therefore, the 65-kDa signal was speculated to be a canine OCT2 [7], but this should be confirmed using an actual antibody against an appropriate antigen. In the present study, we have demonstrated that rOCT2 mediated the uptake of cisplatin into the stable transfectant HEK-rOCT2 cells, and stimulated cisplatin-sensitivity in comparison with the control cells (Figs. 1 and 2). Hitherto it has not been clear which transporter protein mediated the uptake of cisplatin in renal tubular cells. The present study in vitro indicated that rOCT2 was a cisplatin transporter in the kidney.

Intracellularly, the two chlorides of cisplatin are rapidly replaced by hydroxyl groups to produce a toxic agent [21]. This agent can induce nuclear damage [22], cause mitochondrial damage [23] or trigger several other mechanisms [24], resulting in cell death. Therefore, it is considered that the entering into the cells is the most important step in the cytotoxicity of cisplatin. It was reported that the deletion of copper transporter 1 (Ctr1) resulted in resistance to cisplatin in yeast and mammal cells, and therefore, Ctr1 was suggested to be a candidate transporter mediating cisplatin uptake. [25]. On the other hand, copper-transporting P-type adenosine triphosphate (ATP7B) [26–28] and ATP-binding cassette, subfamily C2 (ABCC2, known as MRP2 or cMOAT) [29,30] promoted cisplatin efflux and had a role in cisplatin resistance. However, these three transporters were suggested to have a minor role in cisplatin-induced tubular toxicity, because the tissue distribution of these transporter proteins was not limited to the kidney, but was in the liver, intestine and brain [31–33].

Urakami et al. [18] reported that the renal expression of rOCT2, but not rOCT1, was markedly higher in male than female rats. In addition, there was a gender difference in the uptake of TEA but not *p*-aminohippurate, a typical substrate of organic anion transporter 1, in rat renal slices [18]. Because there is no selective and non-toxic rOCT2 antagonist, we performed the cisplatin pharmacokinetic experiments using the gender difference in the renal rOCT2 expression. It was expected that the renal distribution of cisplatin would be much greater in male than female rats. As expected, the renal CL_{tissue} of cisplatin was significantly greater in male rats than female rats, while hepatic CL_{tissue} did not differ between males and females. Moreover, the renal CL_{tissue} was 3.5 times higher than the hepatic CL_{tissue} in male rats (Fig. 4C). In addition, the transport of cisplatin was mediated by rOCT2 predominantly expressed in kidney [10], but not rOCT1 expressed

in liver, kidney and intestine [34] (Fig. 3C). These results suggested that rOCT2 played a major role in the distribution of cisplatin. As previously reported, the renal clearance of cisplatin was inhibited by cationic compounds having the potential to interact with rOCT2 such as quinidine, cimetidine and ranitidine in dogs [35]. Based on these findings, it was suggested that rOCT2 mainly mediated the tubular accumulation of cisplatin.

There are numerous reports suggesting that cisplatin causes nephrotoxicity, glomerular and tubular injury [3,19,36–38]. In these studies, cisplatin was used at dose of more than 5 mg/kg in rats, which was severe compared to clinical use. The peak concentration of cisplatin in humans undergoing chemotherapy was reported to be 3.4 μg/ml [39]. In the present study, the blood concentration of cisplatin in rats after the administration of cisplatin (0.5 mg/kg) as a bolus was between 1 and 3 μg/ml (Fig. 4A). When rats were administered 2 mg/kg of cisplatin, the activity of NAG in bladder urine and the urine volume were increased, while plasma creatinine level, creatinine clearance, BUN, urinary albumin level, AST, ALT and total bilirubin level were unchanged (Table 1). These results indicated that kidney was more sensitive to cisplatin than liver. It corresponded to the pharmacokinetics of cisplatin (Fig. 4). Kishore et al. [38] demonstrated that the polyuria after the cisplatin treatment was accompanied by decreased expression levels of aquaporin (AQP) 1 in the proximal tubules as well as AQP2 and AQP3 in the collecting ducts in rats. Using the specific antibody, rOCT2 protein was expressed in proximal tubular cells at the basolateral membrane [12] and mRNA of rOCT2 was detected abundantly in proximal tubules and weakly in distal convoluted tubules and collecting ducts [11]. Based on these findings, the proximal tubules were the most sensitive to cisplatin, because they consisted of rOCT2-rich cells.

We previously reported that testosterone increased the expression level of renal rOCT2 and stimulated TEA accumulation by kidney slices [40] and that testosterone recovered the renal rOCT2 expression and the clearance of cimetidine in chronic renal failure rats [41]. In the present study, to investigate the role of rOCT2 in cisplatin-induced tubular toxicity, we used the castrated rats as a model for the depression of rOCT2. As a result, cisplatin induced the increase of urinary NAG activity in the sham-operated rats, but not in the castrated rats whose renal rOCT2 expression was lower than the sham-operated rats (Fig. 5). In addition, cellular uptake and renal distribution of cisplatin depended on rOCT2 expression (Figs. 2B and 4). Therefore, it was suggested that rOCT2 was the determinant of the tissue distribution of cisplatin and cisplatin-induced tubular toxicity in vivo.

The tissue distribution and renal distribution of hOCT2 in humans are similar with those of rats [8,12,13]. The functional characteristics including substrate specificity of hOCT2 was consistent with rOCT2 [9]. Therefore, the present data of rOCT2 on cisplatin-induced nephrotoxicity may be reflected in humans. The renal toxicity of cisplatin in humans should be confirmed in future focusing on hOCT2.

We propose OCT2 as the transporter responsible for cisplatin-induced renal tubular toxicity. Some OCT2-specific antagonists may prevent the nephrotoxicity of cisplatin.

Acknowledgments

This work was supported in part by a grant-in-aid for Research on Advanced Medical Technology from the Ministry of Health, Labor and Welfare of Japan, by a Japan Health Science Foundation "Research on Health Sciences Focusing on Drug Innovation", by a grant-in-aid for Scientific Research from the Ministry of Education, Science, Culture and Sports of Japan, and by the 21st Century COE program "Knowledge Information Infrastructure for Genome Science". A. Yonezawa was supported as a Research Assistant by the 21st Century COE program "Knowledge Information Infrastructure for Genome Science".

Portions of this study were presented as a poster at the 48th Annual Meeting of the Japanese Society of Nephrology, June 23–25, 2005 in Japan and at the 4th International Research Conference of the BioMedical Transporters 2005, August 14–18, 2005 in Switzerland.

References

[1] de Jongh FE, van Veen RN, Veltman SJ, de Wit R, van der Burg ME, van den Bent MJ, et al. Weekly high-dose cisplatin is a feasible treatment option: analysis on prognostic factors for toxicity in 400 patients. Br J Cancer 2003;88:1199–206.
[2] Dobyan DC, Levi J, Jacobs C, Kosek J, Weiner MW. Mechanism of *cis*-platinum nephrotoxicity. II. Morphologic observations. J Pharmacol Exp Ther 1980;213:551–6.
[3] Ichimura T, Hung CC, Yang SA, Stevens JL, Bonventre JV. Kidney injury molecule-1: a tissue and urinary biomarker for nephrotoxicant-induced renal injury. Am J Physiol Renal Physiol 2004;286:F552–3.
[4] Thadhani R, Pascual M, Bonventre JV. Acute renal failure. N Engl J Med 1996;334:1448–60.
[5] Safirstein R, Miller P, Guttenplan JB. Uptake and metabolism of cisplatin by rat kidney. Kidney Int 1984;25:753–8.
[6] Okuda M, Tsuda K, Masaki K, Hashimoto Y, Inui K. Cisplatin-induced toxicity in LLC-PK1 kidney epithelial cells: role of basolateral membrane transport. Toxicol Lett 1999;106:229–35.
[7] Ludwig T, Riethmuller C, Gekle M, Schwerdt G, Oberleithner H. Nephrotoxicity of platinum complexes is related to basolateral organic cation transport. Kidney Int 2004;66:196–202.
[8] Motohashi H, Sakurai Y, Saito H, Masuda S, Urakami Y, Goto M, et al. Gene expression levels and immunolocalization of organic ion transporters in the human kidney. J Am Soc Nephrol 2002;13:866–74.
[9] Inui K, Masuda S, Saito H. Cellular and molecular aspects of drug transport in the kidney. Kidney Int 2000;58:944–58.
[10] Okuda M, Saito H, Urakami Y, Takano M, Inui K. cDNA cloning and functional expression of a novel rat kidney organic cation transporter, OCT2. Biochem Biophys Res Commun 1996;224:500–7.
[11] Urakami Y, Okuda M, Masuda S, Akazawa M, Saito H, Inui K. Distinct characteristics of organic cation transporters, OCT1 and

OCT2. in the basolateral membrane of renal tubules. Pharm Res 2001;18:1528–34.
[12] Sugawara-Yokoo M, Urakami Y, Koyama H, Fujikura K, Masuda S, Saito H, et al. Differential localization of organic cation transporters rOCT1 and rOCT2 in the basolateral membrane of rat kidney proximal tubules. Histochem Cell Biol 2000;114:175–80.
[13] Urakami Y, Okuda M, Masuda S, Saito H, Inui K. Functional characteristics and membrane localization of rat multispecific organic cation transporters, OCT1 and OCT2, mediating tubular secretion of cationic drugs. J Pharmacol Exp Ther 1998;287:800–5.
[14] Urakami Y, Kimura N, Okuda M, Inui K. Creatinine transport by basolateral organic cation transporter hOCT2 in the human kidney. Pharm Res 2004;21:976–81.
[15] Okuda M, Urakami Y, Saito H, Inui K. Molecular mechanisms of organic cation transport in OCT2-expressing Xenopus oocytes. Biochim Biophys Acta 1999;1417:224–31.
[16] Ito T, Yano I, Masuda S, Hashimoto Y, Inui K. Distribution characteristics of levofloxacin and grepafloxacin in rat kidney. Pharm Res 1999;16:534–9.
[17] Masuda S, Saito H, Nonoguchi H, Tomita K, Inui K. mRNA distribution and membrane localization of the OAT-K1 organic anion transporter in rat renal tubules. FEBS Lett 1997;407:127–31.
[18] Urakami Y, Nakamura N, Takahashi K, Okuda M, Saito H, Hashimoto Y, et al. Gender differences in expression of organic cation transporter OCT2 in rat kidney. FEBS Lett 1999;461:339–42.
[19] Horiba N, Masuda S, Takeuchi A, Saito H, Okuda M, Inui K. Gene expression variance based on random sequencing in rat remnant kidney. Kidney Int 2004;66:29–45.
[20] Endo T, Kimura O, Sakata M. Carrier-mediated uptake of cisplatin by the OK renal epithelial cell line. Toxicology 2000;146:187–95.
[21] Goldstein RS, Mayor GH. The nephrotoxicity of cisplatin. Life Sci 1983;32:685–90.
[22] Leibbrandt ME, Wolfgang GH, Metz AL, Ozobia AA, Haskins JR. Critical subcellular targets of cisplatin and related platinum analogs in rat renal proximal tubule cells. Kidney Int 1995;48:761–70.
[23] Zhang JG, Lindup WE. Role of mitochondria in cisplatin-induced oxidative damage exhibited by rat renal cortical slices. Biochem Pharmacol 1993;45:2215–22.
[24] Wang D, Lippard SJ. Cellular processing of platinum anticancer drugs. Nat Rev Drug Discov 2005;4:307–20.
[25] Ishida S, Lee J, Thiele DJ, Herskowitz I. Uptake of the anticancer drug cisplatin mediated by the copper transporter Ctr1 in yeast and mammals. Proc Natl Acad Sci USA 2002;99:14298–302.
[26] Komatsu M, Sumizawa T, Mutoh M, Chen ZS, Terada K, Furukawa T, et al. Copper-transporting P-type adenosine triphosphatase (ATP7B) is associated with cisplatin resistance. Cancer Res 2000;60:1312–6.
[27] Miyashita H, Nitta Y, Mori S, Kanzaki A, Nakayama K, Terada K, et al. Expression of copper-transporting P-type adenosine triphosphatase (ATP7B) as a chemoresistance marker in human oral squamous cell carcinoma treated with cisplatin. Oral Oncol 2003;39:157–62.
[28] Nakayama K, Kanzaki A, Terada K, Mutoh M, Ogawa K, Sugiyama T, et al. Prognostic value of the Cu-transporting ATPase in ovarian carcinoma patients receiving cisplatin-based chemotherapy. Clin Cancer Res 2004;10:2804–11.
[29] Cui Y, Konig J, Buchholz JK, Spring H, Leier I, Keppler D. Drug resistance and ATP-dependent conjugate transport mediated by the apical multidrug resistance protein, MRP2, permanently expressed in human and canine cells. Mol Pharmacol 1999;55:929–37.
[30] Koike K, Kawabe T, Tanaka T, Toh S, Uchiumi T, Wada M, et al. A canalicular multispecific organic anion transporter (cMOAT) antisense cDNA enhances drug sensitivity in human hepatic cancer cells. Cancer Res 1997;57:5475–9.
[31] Zhou B. Gitschier J. hCTR1: a human gene for copper uptake identified by complementation in yeast. Proc Natl Acad Sci USA 1997;94:7481–6.
[32] Buchler M, Konig J, Brom M, Kartenbeck J, Spring H, Horie T, et al. cDNA cloning of the hepatocyte canalicular isoform of the multidrug resistance protein, cMrp, reveals a novel conjugate export pump deficient in hyperbilirubinemic mutant rats. J Biol Chem 1996; 271:15091–8.
[33] Petrukhin K, Lutsenko S, Chernov I, Ross BM, Kaplan JH, Gilliam TC. Characterization of the Wilson disease gene encoding a P-type copper transporting ATPase: genomic organization, alternative splicing, and structure/function predictions. Hum Mol Genet 1994;3: 1647–56.
[34] Grundemann D, Gorboulev V, Gambaryan S, Veyhl M, Koepsell H. Drug excretion mediated by a new prototype of polyspecific transporter. Nature 1994;372:549–52.
[35] Klein J, Bentur Y, Cheung D, Moselhy G, Koren G. Renal handling of cisplatin: interactions with organic anions and cations in the dog. Clin Invest Med 1991;14:388–94.
[36] Chirino YI, Hernandez-Pando R, Pedraza-Chaverri J. Peroxynitrite decomposition catalyst ameliorates renal damage and protein nitration in cisplatin-induced nephrotoxicity in rats. BMC Pharmacol 2004; 4:20.
[37] Jo SK, Cho WY, Sung SA, Kim HK, Won NH. MEK inhibitor, U0126, attenuates cisplatin-induced renal injury by decreasing inflammation and apoptosis. Kidney Int 2005;67:458–66.
[38] Kishore BK, Krane CM, Di Iulio D, Menon AG, Cacini W. Expression of renal aquaporins 1, 2, and 3 in a rat model of cisplatin-induced polyuria. Kidney Int 2004;58:701–11.
[39] Reece PA, Stafford I, Davy M, Freeman S. Disposition of unchanged cisplatin in patients with ovarian cancer. Clin Pharmacol Ther 1987;42:320–5.
[40] Urakami Y, Okuda M, Saito H, Inui K. Hormonal regulation of organic cation transporter OCT2 expression in rat kidney. FEBS Lett 2000; 473:73–6.
[41] Ji L, Masuda S, Saito H, Inui K. Down-regulation of rat organic cation transporter rOCT2 by 5/6 nephrectomy. Kidney Int 2002;62:514–524.

Pharmaceutical Research, Vol. 22, No. 12, December 2005 (© 2005)
DOI: 10.1007/s11095-005-8383-5

Research Paper

Pharmacokinetic Significance of Renal OAT3 (SLC22A8) for Anionic Drug Elimination in Patients with Mesangial Proliferative Glomerulonephritis

Yuji Sakurai,[1] Hideyuki Motohashi,[1] Ken Ogasawara,[1] Tomohiro Terada,[1] Satohiro Masuda,[1] Toshiya Katsura,[1] Noriko Mori,[2] Motokazu Matsuura,[3] Toshio Doi,[3] Atsushi Fukatsu,[4] and Ken-ichi Inui [1,5]

Received July 5, 2005; accepted September 7, 2005

Purpose. Our previous studies showed that the mRNA level of human organic anion transporter (hOAT) 3 in the kidney was correlated with the rate of elimination of an anionic antibiotic cefazolin. However, the correlation coefficient was not so high. In the present study, therefore, we enrolled more patients to examine whether additional factors were responsible for the correlation.
Methods. hOAT mRNA levels in renal biopsy specimens were quantified using the real-time polymerase chain reaction method. The elimination rates for the free fraction of cefazolin were determined in patients with various renal diseases.
Results. In the present study, the coefficient of correlation between the hOAT3 mRNA level and the elimination rates for the free fraction of cefazolin was not so high in the patients overall as in our previous study ($r = 0.536$). However, following the classification of renal diseases, a better correlation was obtained in patients with mesangial proliferative glomerulonephritis ($r = 0.723$). In contrast, multiple regression analyses including gender, age, and liver function did not result in any improvements in the correlation coefficients.
Conclusions. These results suggest that the hOAT3 mRNA level is a significant marker of pharmacokinetics with which to predict the rate of elimination of cefazolin in patients with mesangial proliferative glomerulonephritis.

KEY WORDS: organic anion transporter; human kidney; renal diseases; real-time PCR; renal clearance.

INTRODUCTION

In patients with renal impairment, individualized dosages are adjusted by using the plasma creatinine concentration or creatinine clearance (C_{cr}) to avoid adverse effects (1). C_{cr} is often used to estimate the glomerular filtration rate (GFR), because creatinine is mainly eliminated via glomerular filtration. However, C_{cr} would not reflect the true GFR, especially in patients with renal impairment, because the amount of tubular secretion is the negligible part of urinary excretion of creatinine (2). Recently, organic cation transporter (OCT) 2 (SLC22A2) was reported to transport creatinine suggesting that OCT2 plays an important role in the secretion of creatinine (3). Furthermore, accumulating evidence shows a poor correlation between C_{cr} and the urinary excretion of drugs (4,5), challenging the "intact nephron hypothesis" and suggesting that the renal handling of drugs may not decline in parallel. Therefore, it is necessary to identify more reliable markers to predict renal function such as the tubular secretion of drugs.

The renal handling of drugs involves three processes: glomerular filtration, tubular secretion, and reabsorption. Tubular secretion and reabsorption are mediated by various transporters expressed in the apical and basolateral membranes of the tubular epithelial cells (6,7). The organic anion transporters (OATs, SLC22A) can transport many ionic drugs and are expressed in the renal proximal tubules (8,9). However, the pharmacokinetic significance of each transporter in the clinical setting has not been fully elucidated.

Previously, we quantified the expression of hOAT1–4 mRNA and urinary excretion of the anionic antibiotic cefazolin in patients with renal diseases. The mRNA level of hOAT3, among the four anion transporters, significantly correlated with the rate of elimination of cefazolin ($n = 42$; $r = 0.44$, $p < 0.01$) (10). In addition, hOAT3 transported cefazolin. The renal expression level of hOAT3 possibly affects the renal handling of cefazolin. However, the coefficient of correlation between the hOAT3 mRNA level and elimination rate of cefazolin was not so high. Therefore, it is postulated that additional factors affect this coefficient.

[1] Department of Pharmacy, Kyoto University Hospital, Faculty of Medicine, Kyoto University, Sakyo-ku, Kyoto, Japan.
[2] Department of Nephrology, Shizuoka Prefectural Hospital, Shizuoka, Japan.
[3] Department of Clinical Biology and Medicine, Course of Biological Medicine, School of Medicine, University of Tokushima, Tokushima, Japan.
[4] Division of Artificial Kidneys, Kyoto University Hospital, Faculty of Medicine, Kyoto University, Kyoto, Japan.
[5] To whom correspondence should be addressed. (e-mail: inui@kuhp.kyoto-u.ac.jp)

0724-8741/05/1200-2016/0

In our previous report, patients with various renal diseases were studied without classification. Because the cause and pathway of progression vary with the type of renal disease (11–13), proximal tubules may be exposed to different regulatory factors depending on the disease. In the present study, we enrolled more patients to examine whether the type of renal disease is a factor in the correlation between the hOAT3 mRNA level and the rate of elimination of cefazolin.

MATERIALS AND METHODS

Patients

A total of 75 patients were enrolled in the study (44 males and 31 females) aged 16–90 years (mean ± SD, 42.4 ± 18.5) with histopathologically confirmed renal disease. Patient profiles are described in Table I. Patients with mesangial proliferative GN (n = 38; 22 males and 16 females, aged 39.8 ± 18.4 years), which is recognized as the most common form of primary renal disease, were categorized as Group I. Those with other renal diseases (n = 37; 22 males and 15 females, aged 45.1 ± 18.5 years) were categorized into Group II. In Group II, eight patients had membranous nephropathy, eight had minimal change nephritic syndrome, seven had lupus nephritis, four had diabetic nephropathy, three had membranoproliferative GN, and seven had other renal diseases. Clinical tests, such as measurements of C_{cr} or 120-min values of the phenolsulfonphthalein (PSP) test (PSP120′), were routinely conducted in the hospital to evaluate renal function. This study was conducted in accordance with the Declaration of Helsinki, and its amendments and was approved by the Kyoto University Graduate School and Faculty of Medicine, Ethics Committee. All patients gave written informed consent to participate in the study.

Isolation of total RNA and genomic DNA

Total RNA from renal biopsy specimens and genomic DNA from blood in a guanidinium thiocyanate solution were isolated with a MagNA Pure LC RNA isolation Kit II and DNA isolation Kit I (Roche Diagnostic, Mannheim, Germany), respectively. Total RNA was reverse-transcribed in the presence of RTmate solution (Wako Pure Chemical Industries, Osaka, Japan), and the single-stranded DNA was used for quantification of mRNA levels.

Quantification of mRNA levels

The mRNA levels of hOAT1–4 were quantified as described previously (14). Using single-stranded DNA (ssDNA), a real-time polymerase chain reaction (PCR) was performed using the ABI Prism 7700 sequence detector (Applied Biosystems, Foster City, CA, USA). Reactions were carried out in duplicate under identical conditions. Glyceraldehyde-3-phosphate dehydrogenase (GAPDH) mRNA was also quantified as an internal control using GAPDH Control Reagent (Applied Biosystems).

Measurement of Elimination Rate Constant for Free Fraction of Cefazolin

After renal biopsy, the patients received 1 g of cefazolin by intravenous infusion for 1 h as a prophylaxis of infection. Collection of blood samples and measurement of cefazolin concentrations by high-performance liquid chromatography (HPLC) were carried out as previously described (10). The plasma unbound fraction (fu) of cefazolin was determined by ultrafiltration using a micropartition system (MRS-1; Amicon, Inc., Beverly, MA, USA) (15). Free fraction of cefazolin was expressed as the ratio of the concentration in ultrafiltrate to that in plasma. The apparent elimination rate constant of the free fraction ($Ke_{free,cez}$) was calculated using the free fraction of the plasma cefazolin concentration immediately and 1 h after cefazolin infusion.

Genotyping of the *hOAT3* gene

The genotypes of the *hOAT3* gene—C715T (Gln239Stop), T779G (Ile260Arg), C829T (Arg277Trp), A913T (Ile305Phe), C929T (Ala310Val), and G1342A (Val448Ile), which were reported in the public single nucleotide polymorphisms (SNPs) database NCBI dbSNP—were examined via the PCR restriction enzyme

Table I. Characteristics of Patients with Renal Disease

	All patients	Group I	Group II	p Value
No. of patients	75	38	37	
Sex (males/females)	44/31	22/16	22/15	
Age	42.4 ± 18.5	39.8 ± 18.4	45.1 ± 18.5	0.221
Aspartate aminotransferase (IU/L)	19.6 ± 8.9	18.3 ± 6.9	20.9 ± 10.6	0.232
Alanine aminotransferase (IU/L)	16.7 ± 10.1	14.9 ± 7.2	18.7 ± 12.2	0.113
Lactate dehydrogenase (mg/L)	180.5 ± 52.8	171.3 ± 51.6	190.3 ± 53.1	0.139
Serum creatinine (mg/dL)	1.1 ± 0.6	1.1 ± 0.7	1.0 ± 0.5	0.503
Uric acid (mg/dL)	6.3 ± 1.5	6.1 ± 1.4	6.4 ± 1.6	0.442
Blood urea nitrogen (mg/dL)	17.6 ± 11.1	16.4 ± 8.0	18.8 ± 13.5	0.341
Creatinine clearance (mL/min)	63.2 ± 28.1	64.6 ± 29.4	61.8 ± 27.0	0.672
PSP120′ (%)	64.9 ± 20.4	65.9 ± 18.7	63.4 ± 22.7	0.652
$Ke_{free\ cez}$	0.74 ± 0.25	0.73 ± 0.26	0.75 ± 0.25	0.619

Group I includes the patients with mesangial proliferative glomerulonephritis. All other patients were categorized in Group II.
Variance is indicated as the mean ± SD.
p Values are for the comparison between Group I and Group II.

Table II. Primer Sets for PCR-RFLP

Position of mutation		Primer sequences	Restriction enzyme
cDNA715	Forward	5′-CCTGGGACCTAGCAGAACACTA-3′	*Pst*I
	Reverse	5′-TGAAGAGGAGAGGGCCACAT-3′	
cDNA779	Forward	5′-CTGTTGATGTTCTTCCAGCCTCTCA-3′	*Nde*I
	Reverse	5′-TCCAGACAAGACCAACCAGCAT-3′	
cDNA829	Forward	5′-CTGTTGATGTTCTTCCAGCCTCTCA-3′	*Bsp*EI
	Reverse	5′-ATTGAAGACAGCCACCCTCC-3′	
cDNA913	Forward	5′-TAGAGGCACCACGCCTGCAT-3′	*Bgl*II
	Reverse	5′-GGTTACCAGGCCAGGGAAAGA-3′	
cDNA929	Forward	5′-TAGAGGCACCACGCCTGCAT-3′	*Stu*I
	Reverse	5′-GGAACAGGTCACTTGCGGTGTACTAG-3′	
cDNA1342	Forward	5′-CAGGTGGGACTGTGGCATTGT-3′	*Bsi*WI
	Reverse	5′-ACGCGGGTCCACAGGTTACGTA-3′	

fragment length polymorphism (RFLP) method in 67 patients. Genomic DNA could not be obtained from eight patients, who consented to the mRNA quantification and pharmacokinetic study but refused more genetic analyses. The specific primers and restriction enzymes used in this study are listed in Table II. The PCR conditions were as follows: after denaturing at 94°C for 3 min, PCR was performed with 1 μM of each primer and *Taq* DNA polymerase (Takara, Shiga, Japan), according to the following profile—94°C for 1min, 63°C for 1min, and 72°C for 1min, 35 cycles, followed by a single additional 10-min extension at 72°C. The PCR products were digested with or without apparent restriction enzymes and separated by electrophoresis on 3% agarose gel. The sequence of the *hOAT3* polymorphism (A/T913 corresponding to Ile305Phe) was confirmed by direct sequencing in heterozygotes using a multicapillary DNA sequencer RISA384 system (Shimadzu, Kyoto, Japan).

Statistical Analysis

Simple and multiple regression analyses were performed using the least-squares method. Multiple regression analyses were performed to determine the impact of the patient's characteristics on the correlation between the logarithmically transformed hOAT3 mRNA data and $Ke_{free,cez}$ or the 120-min values of the PSP test (PSP120′). In multiple regression analyses, we used $Ke_{free,cez}$ or PSP120′ as the outcome variable, and the hOAT3 mRNA level and parameters of patients as predictor variables. The nonpaired Student *t* test was used to compare groups. Statistical analyses were performed with Stat View, version 5.0 (Abacus Concepts, Berkeley, CA, USA).

Materials and Methods

Cefazolin was kindly provided by Fujisawa Pharmaceutical Co. Ltd. (Osaka, Japan). All other chemicals used were of the highest purity available.

RESULTS

The coefficient of correlation between $Ke_{free,cez}$ and C_{cr} was 0.439 ($p < 0.01$), and between $Ke_{free,cez}$ and PSP120′ it was 0.705 ($p < 0.01$) (Fig. 1A and B). As in the previous study, it was confirmed that hOAT3 mRNA level was significantly correlated with $Ke_{free,cez}$ ($r = 0.536$; $p < 0.01$) (Fig. 1C). In addition, a significant correlation between hOAT3 mRNA level and PSP120′ ($r = 0.484$; $p < 0.01$) was found (Fig. 1D).

To investigate whether the type of renal disease affects the correlation, patients were divided into Groups I (mesangial proliferative GN) and II (other renal diseases). As shown in Table I, there were no significant differences in the population between the two groups. In addition, $Ke_{free,cez}$ was significantly correlated with PSP120′ ($r = 0.723$, $p < 0.01$; Group I, $r = 0.713$, $p < 0.01$; Group II) more than C_{cr} ($r =$

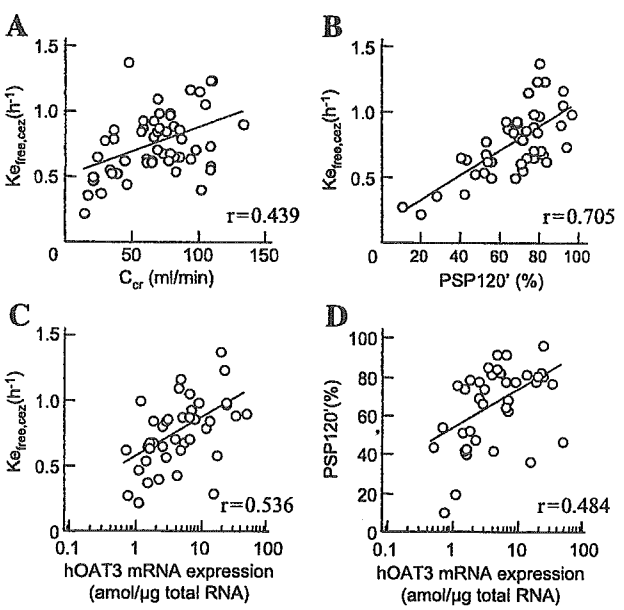

Fig. 1. The linear regression of creatinine clearance (C_{cr}) (A) or the 120-min values of the phenolsulfonphthalein test (PSP120′) (B) against the elimination rate constant for the free fraction of cefazolin ($Ke_{free,cez}$), and the linear regression between hOAT3 mRNA levels and $Ke_{free,cez}$ (C) or PSP120′ (D) in patients with renal diseases. The plasma concentration of cefazolin was measured by HPLC, and $Ke_{free,cez}$ was calculated. Total cellular RNA was extracted from the kidney biopsy specimens. The mRNA levels of hOAT3 were quantified by real-time PCR.

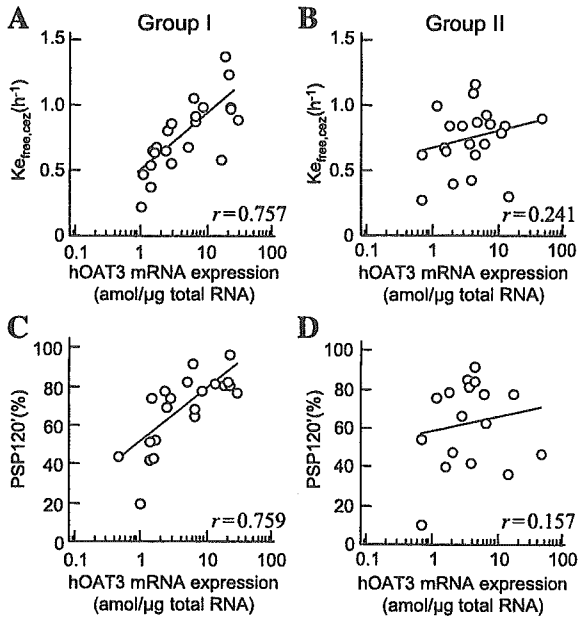

Fig. 2. The linear regression of hOAT3 mRNA levels against $Ke_{free,cez}$ (A, B) or PSP120′ (C, D) in Group I (A, C) or Group II (B, D). The plasma concentration of cefazolin was measured by HPLC, and $Ke_{free,cez}$ was calculated. Total cellular RNA was extracted from the renal biopsy specimens. The mRNA levels of hOAT3 were quantified by real-time PCR.

0.492, $p < 0.01$; Group I, $r = 0.474$, $p < 0.05$; Group II) in both groups.

Figure 2A and B shows the results of linear regression analyses with mRNA level of hOAT3 and $Ke_{free,cez}$. In Group I, the coefficient of correlation between hOAT3 mRNA level and $Ke_{free,cez}$ ($r = 0.757$; $p < 0.01$) was much higher than that in all patients. On the other hand, $Ke_{free,cez}$ was independent of hOAT3 mRNA level in Group II ($r = 0.241$; $p = 0.296$). Table III summarizes the coefficients of correlation between hOAT1–4 mRNA levels and $Ke_{free,cez}$ in each group. Although the expression level of hOAT1 mRNA was correlated with $Ke_{free,cez}$ in Group I, its coefficient was lower than the value for hOAT3. In Group II, there were no correlations between hOAT1–4 mRNA levels and $Ke_{free,cez}$. The same results were obtained between hOAT1–4 mRNA levels and PSP120′ (Fig. 2C and D, Table III).

Table III. Correlation Coefficients for $Ke_{free,cez}$, PSP120′, and the Expression Levels of hOAT mRNAs in Group I and Group II

	Group I		Group II	
mRNA expression	$Ke_{free,cez}$	PSP120′	$Ke_{free,cez}$	PSP120′
hOAT1	0.558[a]	0.556[a]	0.267	0.391
hOAT2	0.051	0.083	0.387	0.213
hOAT3	0.757[a]	0.759[a]	0.241	0.157
hOAT4	0.183	0.186	0.247	0.474

Values represent coefficients of the correlation between mRNA expression of hOATs and $Ke_{free,cez}$ or PSP120′.
[a] Each mRNA level of hOAT is significantly correlated with $Ke_{free,cez}$ or PSP120′.

Table IV. Multiple Regression Analyses for $Ke_{free,cez}$ or PSP120′

	r Value	
+ Additional parameters	$Ke_{free,cez}$	PSP120′
hOAT3 mRNA level + age	0.603	0.526
hOAT3 mRNA level + aspartate aminotransferase	0.585	0.558
hOAT3 mRNA level + alanine aminotransferase	0.543	0.534
hOAT3 mRNA level + lactate dehydrogenase	0.530	0.497

To assess whether personal profiles of patients and liver functions affect the correlation between hOAT3 mRNA level and $Ke_{free,cez}$, simple or multiple linear regression analyses were performed using gender, age, aspartate aminotransferase (AST), alanine aminotransferase (ALT), and lactate dehydrogenase (LDH). Coefficients of correlation were not improved by dividing the subjects into males and females ($r = 0.450$, $p < 0.01$; males, $r = 0.600$, $p < 0.01$; females). Table IV shows the results of multiple linear regression analyses. Age and liver functions did not improve the correlation. In addition, the same results were observed for PSP120′.

Next, we investigated six SNPs in coding regions (cSNPs) with nonsynonymous changes in the *hOAT3* gene of 67 patients, because some cSNPs in the *hOAT3* gene were considered to affect the transport activity independent of the expression level. In the *hOAT3* gene, one nonsynonymous polymorphism (A913 was replaced with T) was detected via the PCR-RFLP method and confirmed by direct sequencing (Table V, Fig. 3). This polymorphism resulted in an amino acid substitution; Ile305 was changed to Phe (Ile305Phe). The allele frequency of cDNA 913 was 95.5% for allele A and 4.5% for allele T. However, there was no remarkable difference in $Ke_{free,cez}$ or PSP120′ between the two genotypic groups (Table V). Furthermore, the coefficient of correlation between hOAT3 mRNA level and $Ke_{free,cez}$ ($r = 0.551$, $p < 0.01$) or PSP120′ ($r = 0.493$, $p < 0.01$) was not changed by excluding patients with this variant.

DISCUSSION

Recent insights into the mechanisms of progressive renal dysfunction have indicated that tubulointerstitial pathology does not simply follow glomerular injury and that tubular cells may be the primary targets for various pathophysiological influences (16). Among each type of renal disease, the cause and pathway of progression are different (11–13). For each type of renal disease, renal transporters are assumed regulated in a different manner. Therefore, it may be important to consider types of renal disease when assessing the correlation between pharmacokinetics and expression levels of transporters. In the present study, we found a good relationship between the hOAT3 mRNA level and the rate of elimination of cefazolin in patients with mesangial proliferative GN (Group I), which is the most common form of primary renal disease (17). It was postulated that hOAT3 expression levels directly regulated the rate of elimination of

Table V. hOAT3 Genetic Variants in Patients with Renal Diseases and Phenotypic Indexes (n = 67)

Location	Position	Allele	Effect	Allele frequency	Genotype	Frequency (%)	$Ke_{free,cez}$ (h^{-1})	PSP120′ (%)
Exon5	cDNA715	C	239Gln	67 (100.0%)	C/C	100.0		
		T	239Stop	0 (0.0%)	C/T	0.0		
					T/T	0.0		
Exon6	cDNA779	T	260Ile	67 (100.0%)	T/T	100.0		
		G	260Arg	0 (0.0%)	T/G	0.0		
					G/G	0.0		
Exon6	cDNA829	C	277Arg	67 (100.0%)	C/C	100.0		
		T	277Trp	0 (0.0%)	C/T	0.0		
					T/T	0.0		
Exon7	cDNA913	A	305Ile	64 (100.0%)	A/A	91.0	0.75 ± 0.25	66.1 ± 20.5
		T	305Phe	3 (4.5%)	A/T	9.0	0.84 ± 0.29	64.2 ± 15.6
					T/T	0.0		
Exon7	cDNA929	C	310Ala	67 (100.0%)	C/C	100.0		
		T	310Val	0 (0.0%)	C/T	0.0		
					T/T	0.0		
Exon10	cDNA1342	G	448Val	67 (100.0%)	G/G	100.0		
		A	448Ile	0 (0.0%)	G/A	0.0		
					A/A	0.0		

Variance is indicated as the mean ± SD.

cefazolin in these patients. The level of hOAT1 mRNA was also correlated with $Ke_{free,cez}$ in Group I. However, its correlation coefficient was lower than the coefficient between hOAT3 mRNA levels and $Ke_{free,cez}$. In addition, transport of cefazolin by hOAT1 was negligible in our previous study (10,18). Therefore, it was considered that elimination rate of cefazolin was affected by the expression level of hOAT3 rather than hOAT1.

On the other hand, in Group II, there was no significant correlation between the mRNA level of hOAT3 and the rate of elimination of cefazolin. It is suggested that additional factors are affecting the rate. One possibility is that hOAT3 is regulated by a posttranslational mechanism in these patients. For example, the activation of protein kinase C (PKC) inhibited the uptake of anionic compounds by OAT3 in intact renal proximal tubules and cells stably expressing OAT3 (19). It was recently reported by Soodvilai *et al.* (20,21) that tyrosine kinase, phosphatidylinositol 3-kinase, mitogen-activated protein kinase, protein kinase A, and mitogen-activated/extracellular signal-regulated kinase kinase were involved in epidermal growth factor signaling pathways, which could affect the function of OAT3. Group II included patients with diabetic nephropathy, and the PKC activity of renal tubular cells was reported to be increased in the diabetic state (22,23). Thus, it is possible that the function of hOAT3 is modified by various kinases in some patients of Group II. However, the signaling pathways in proximal tubules specific for each renal disease, such as lupus nephritis or interstitial nephritis, are little understood in contrast to those in the glomeruli. Further studies should be performed to clarify the posttranslational regulation of tubular transporters in renal disease.

Poor correlations between C_{cr} and the renal clearance of drugs have been reported (4,5). In the present study, C_{cr} was not a good predictor of $Ke_{free,cez}$ (Fig. 1), indicating that C_{cr} can not be used to accurately assess anionic drug excretion. Alternatively, it has been indicated that tubular function should be considered when making precise adjustments of dosage. However, tubular function is not routinely evaluated in the clinical setting. In the present study, hOAT3 mRNA level was significantly correlated with PSP120′ in the patients with mesangial proliferative GN (Fig. 2). PSP is almost completely excreted into urine in the unchanged form (24,25) and in a substrate of hOAT3 (10). It is suggested that PSP tests are good predictors of the renal elimination rate of drugs, which are transported by hOAT3, with less invasive methods. Markers for the expression level of individual transporters from urine or blood will be useful to predict the rate of elimination of substrate drugs.

Genetic polymorphisms of drug transporters as well as drug-metabolizing enzymes affect the pharmacokinetics of drugs. Ishikawa *et al.* (26) suggested that cSNPs of transporter genes are responsible for the variation in responses to drugs among individuals. For example, SNPs of human organic anion transporting polypeptides (OATP-C, SLC21A6) were reported to influence the pharmacokinetics of pravastatin (27–29). In the present study, we screened for six cSNPs of the *hOAT3* gene, and found one polymorphism, Ile305Phe (allelic frequency, 4.5%). However, no pharmacokinetic significance of this cSNP was apparent. Nishizato *et al.* (28) also reported that a polymorphism in the *hOAT3* gene,

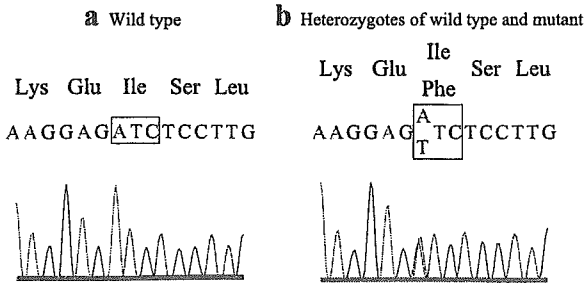

Fig. 3. Electropherograms of the SLC22A8 gene sequence in the region around the A913T mutation.

T723A (Ala389Val), was unlikely to be associated with differences in the clearance of pravastatin. Thus, it is likely that cSNPs of *hOAT3* do not account for variation in the rate of elimination in most cases, and that the expression level of hOAT3 is more important to explain the interindividual variation in the elimination rates of cefazolin and PSP than cSNPs in patients with renal diseases.

There are several differences in substrate specificity between hOAT1 and hOAT3. hOAT3, but not hOAT1, transports estrone sulfate (ES), and the cationic drug famotidine (30,31). Renal elimination rates of these substrates may also be affected by hOAT3 expression levels. While methotrexate was transported by both hOAT1 and hOAT3 (32), aciclovir and ganciclovir were transported by hOAT1 but not hOAT3 (33). It is assumed that the urinary excretion of these drugs is affected by hOAT1 expression levels.

In conclusion, the expression level of hOAT3 mRNA was suggested to be a significant pharmacokinetics marker in predicting the rate of elimination of anionic drugs in patients with mesangial proliferative GN.

ACKNOWLEDGMENTS

This work was supported by a grant-in-aid for Comprehensive Research on Aging and Health from the Ministry of Health and Welfare of Japan (H15-Choju-006), by a grant-in-aid for Scientific Research from the Ministry of Education, Culture, Sports, Science, and Technology of Japan, by a grant-in-aid from the Japan Research Foundation for Clinical Pharmacology, and by the 21st Century COE program "Knowledge Information Infrastructure for Genome Science."

REFERENCES

1. L. Dettli. Drug dosage in renal disease. *Clin. Pharmacokinet.* **1**:126–134 (1976).
2. O. Shemesh, H. Golbetz, J. P. Kriss, and B. D. Myers. Limitations of creatinine as a filtration marker in glomerulopathic patients. *Kidney Int.* **28**:830–838 (1985).
3. Y. Urakami, N. Kimura, M. Okuda, and K. Inui. Creatinine transport by basolateral organic cation transporter hOCT2 in the human kidney. *Pharm. Res.* **21**:976–981 (2004).
4. R. Hori, K. Okumura, A. Kamiya, H. Nihira, and H. Nakano. Ampicillin and cephalexin in renal insufficiency. *Clin. Pharmacol. Ther.* **34**:792–798 (1983).
5. S. E. Tett, C. M. Kirkpatrick, A. S. Gross, and A. J. McLachlan. Principles and clinical application of assessing alterations in renal elimination pathways. *Clin. Pharmacokinet.* **42**:1193–1211 (2003).
6. J. B. Pritchard and D. S. Miller. Mechanisms mediating renal secretion of organic anions and cations. *Physiol. Rev.* **73**:765–796 (1993).
7. K. Inui and M. Okuda. Cellular and molecular mechanisms of renal tubular secretion of organic anions and cations. *Clin. Exp. Nephrol.* **2**:100–108 (1998).
8. K. Inui, S. Masuda, and H. Saito. Cellular and molecular aspects of drug transport in the kidney. *Kidney Int.* **58**:944–958 (2000).
9. B. C. Burckhardt and G. Burckhardt. Transport of organic anions across the basolateral membrane of proximal tubule cells. *Rev. Physiol., Biochem. Pharmacol.* **146**:95–158 (2003).
10. Y. Sakurai, H. Motohashi, H. Ueo, S. Masuda, H. Saito, M. Okuda, N. Mori, M. Matsuura, T. Doi, A. Fukatsu, O. Ogawa, and K. Inui. Expression levels of renal organic anion transporters (OATs) and their correlation with anionic drug excretion in patients with renal diseases. *Pharm. Res.* **21**:61–67 (2004).
11. R. E. Gilbert and M. E. Cooper. The tubulointerstitium in progressive diabetic kidney disease: more than an aftermath of glomerular injury? *Kidney Int.* **56**:1627–1637 (1999).
12. M. H. Park, V. D'Agati, G. B. Appel, and C. L. Pirani. Tubulointerstitial disease in lupus nephritis: relationship to immune deposits, interstitial inflammation, glomerular changes, renal function, and prognosis. *Nephron* **44**:309–319 (1986).
13. E. Alexopoulos, D. Seron, R. B. Hartley, and J. S. Cameron. Lupus nephritis: correlation of interstitial cells with glomerular function. *Kidney Int.* **37**:100–109 (1990).
14. H. Motohashi, Y. Sakurai, H. Saito, S. Masuda, Y. Urakami, M. Goto, A. Fukatsu, O. Ogawa, and K. Inui. Gene expression levels and immunolocalization of organic ion transporters in the human kidney. *J. Am. Soc. Nephrol.* **13**:866–874 (2002).
15. I. Yano, T. Ito, M. Takano, and K. Inui. Evaluation of renal tubular secretion and reabsorption of levofloxacin in rats. *Pharm. Res.* **14**:508–511 (1997).
16. K. A. Nath. The tubulointerstitium in progressive renal disease. *Kidney Int.* **54**:992–994 (1998).
17. J. Floege and J. Feehally. IgA nephropathy: recent developments. *J. Am. Soc. Nephrol.* **11**:2395–2403 (2000).
18. H. Ueo, H. Motohashi, T. Katsura, K. Inui. Human organic anion transporter hOAT3 is a potent transporter of cephalosporin antibiotics, in comparison with hOAT1. *Biochem. Pharmacol.* **70**:1104–1113 (2005).
19. M. Takeda, T. Sekine, and H. Endou. Regulation by protein kinase C of organic anion transport driven by rat organic anion transporter 3 (rOAT3). *Life Sci.* **67**:1087–1093 (2000).
20. S. Soodvilai, V. Chatsudthipong, K. K. Evans, S. H. Wright, and W. H. Dantzler. Acute regulation of OAT3-mediated estrone sulfate transport in isolated rabbit renal proximal tubules. *Am. J. Physiol. Renal. Physiol.* **287**:F1021–F1029 (2004).
21. S. Soodvilai, S. H. Wright, W. H. Dantzler, V. Chatsudthipong. Involvement of tyrosine kinase and PI3K in the regulation of OAT3-mediated estrone sulfate transport in isolated rabbit renal proximal tubules. *Am. J. Physiol. Renal. Physiol.* in press.
22. D. Koya and G. L. King. Protein kinase C activation and the development of diabetic complications. *Diabetes* **47**:859–866 (1998).
23. S. H. Park, H. J. Choi, J. H. Lee, C. H. Woo, J. H. Kim, and H. J. Han. High glucose inhibits renal proximal tubule cell proliferation and involves PKC, oxidative stress, and TGF-beta 1. *Kidney Int.* **59**:1695–1705 (2001).
24. J. V. Moller and M. I. Sheikh. Renal organic anion transport system: pharmacological, physiological, and biochemical aspects. *Pharmacol. Rev.* **34**:315–358 (1982).
25. G. R. Brown. Cephalosporin–probenecid drug interactions. *Clin. Pharmacokinet.* **24**:289–300 (1993).
26. T. Ishikawa, A. Tsuji, K. Inui, Y. Sai, N. Anzai, M. Wada, H. Endou, and Y. Sumino. The genetic polymorphism of drug transporters: functional analysis approaches. *Pharmacogenomics* **5**:67–99 (2004).
27. C. Marzolini, R. G. Tirona, and R.B. Kim. Pharmacogenomics of the OATP and OAT families. *Pharmacogenomics* **5**:273–282 (2004).
28. Y. Nishizato, I. Ieiri, H. Suzuki, M. Kimura, K. Kawabata, T. Hirota, H. Takane, S. Irie, H. Kusuhara, Y. Urasaki, A. Urae, S. Higuchi, K. Otsubo, and Y. Sugiyama. Polymorphisms of OATP-C (SLC21A6) and OAT3 (SLC22A8) genes: consequences for pravastatin pharmacokinetics. *Clin. Pharmacol. Ther.* **73**:554–565 (2003).
29. M. Niemi, E. Schaeffeler, T. Lang, M. F. Fromm, M. Neuvonen, C. Kyrklund, J. T. Backman, R. Kerb, M. Schwab, P. J. Neuvonen, M. Eichelbaum, and K. T. Kivisto. High plasma pravastatin concentrations are associated with single nucleotide polymorphisms and haplotypes of organic anion transporting polypeptide-C (OATP-C, SLCO1B1). *Pharmacogenetics* **14**:429–440 (2004).
30. S. H. Cha, T. Sekine, J. I. Fukushima, Y. Kanai, Y. Kobayashi,

T. Goya, and H. Endo. Identification and characterization of human organic anion transporter 3 expressing predominantly in the kidney. *Mol. Pharmacol.* **59**:1277–1286 (2001).
31. H. Motohashi, Y. Uwai, K. Hiramoto, M. Okuda, and K. Inui. Different transport properties between famotidine and cimetidine by human renal organic ion transporters (SLC22A). *Eur. J. Pharmacol.* **503**:25–30 (2004).
32. Y. Uwai, R. Taniguchi, H. Motohashi, H. Saito, M. Okuda, and K. Inui. Methotrexate–loxoprofen interaction: involvement of human organic anion transporters hOAT1 and hOAT3. *Drug Metab. Pharmacokinet.* **19**:369–374 (2004).
33. M. Takeda, S. Khamdang, S. Narikawa, H. Kimura, Y. Kobayashi, T. Yamamoto, S. H. Cha, T. Sekine, and H. Endou. Human organic anion transporters and human organic cation transporters mediate renal antiviral transport. *J. Pharmacol. Exp. Ther.* **300**:918–924 (2002).

Pflugers Arch - Eur J Physiol (2006) 452: 64–70
DOI 10.1007/s00424-005-0005-x

EPITHELIAL TRANSPORT

Megumi Irie · Tomohiro Terada · Masahiro Tsuda · Toshiya Katsura · Ken-ichi Inui

Prediction of glycylsarcosine transport in Caco-2 cell lines expressing PEPT1 at different levels

Received: 20 June 2005 / Accepted: 22 September 2005 / Published online: 10 November 2005

Abstract H^+-coupled peptide transporter 1 (PEPT1) and the basolateral peptide transporter mediate the absorption of small peptides and peptide-like drugs in the small intestine. Recently, we constructed a mathematical model to simulate glycylsarcosine (Gly-Sar) transport in Caco-2 cells. In this study, we attempted to adjust our model to a change in the expression level of PEPT1. To obtain cell lines expressing PEPT1 at different levels, recloning of Caco-2 cells was performed, and nine clones were isolated. Compared with parental cells, clones 1 and 9 exhibited the lowest and the highest levels of [^{14}C]Gly-Sar uptake from the apical side, respectively, whereas activities of the basolateral peptide transporter were comparable. Kinetic analysis demonstrated that the difference in the activity of PEPT1 was accounted by variations in V_{max}. Moreover, PEPT1 mRNA level was positively related to the activity of [^{14}C]Gly-Sar uptake (r=0.55). Based on these findings, the V_{max} value of PEPT1 was defined as a variable using the amount of PEPT1 mRNA as an index of the expression level. With this improved model, Gly-Sar transport in clones 1 and 9 was well-predicted, suggesting that our model can simulate Gly-Sar transport in cells expressing PEPT1 at different levels.

Keywords Peptide transporter · Small intestine · Absorption · Simulation · Expression level

Abbreviations PEPT1: H^+-coupled peptide transporter 1 · Gly-Sar: glycylsarcosine

M. Irie · T. Terada · M. Tsuda · T. Katsura · K.-i. Inui (✉)
Department of Pharmacy,
Kyoto University Hospital,
Faculty of Medicine,
Kyoto University,
Sakyo-ku,
606-8507 Kyoto, Japan
e-mail: inui@kuhp.kyoto-u.ac.jp
Tel.: +81-75-7513577
Fax: +81-75-7514207

Introduction

H^+-coupled peptide transporter 1 (PEPT1) expressed in brush-border membranes of intestinal epithelial cells transports dipeptides and tripeptides from the lumen into cells by utilizing an inward H^+ gradient and mediates the absorption of dipeptides and tripeptides [1, 6, 14, 23]. Because of its broad substrate specificity, PEPT1 can accept various peptide-like drugs, such as oral β-lactam antibiotics and the anticancer agent bestatin; therefore, PEPT1 serves as a drug transporter [7, 23, 29]. On the other hand, it has been demonstrated that another peptide transporter is expressed in the basolateral membrane [10, 12, 19, 24, 26, 27]. The basolateral peptide transporter mediates the extrusion of substrates taken up by PEPT1 into the circulation and is involved in the absorption of peptide-like drugs.

Recently, based on the influx and efflux properties of PEPT1 and the basolateral peptide transporter, we constructed a computational model of glycylsarcosine (Gly-Sar) transport in Caco-2 cells [11]. This model was composed of three compartments (i.e., the apical, cellular, and basolateral compartments) and two functional factors (PEPT1 and the basolateral peptide transporter). To reproduce the saturation of both transporters, the rate constants of Gly-Sar transport by PEPT1 and the basolateral peptide transporter were defined as variables using the respective kinetic parameters K_m and V_{max}. With this model, the time course of Gly-Sar transport at various concentrations in the absorptive direction could be predicted well, indicating that the model could be used to underlie a simulator to forecast the absorption of peptide-like drugs in the small intestine. However, the expression level of PEPT1 was presumed to be constant and was not incorporated into this model as a variable factor, although the expression level of PEPT1 differed from the segment of the intestine [17] and the intestinal PEPT1 was regulated by various factors, such as food, hormones, drugs, and diurnal rhythm [2, 23]. It is, therefore, essential to enable the model to achieve a change in the expression level of PEPT1 for the development of a simulator of drug absorption in the small intestine.

In the present study, we first performed the recloning of Caco-2 cells for two purposes: (1) to isolate clones appropriate for assessment of the improved model, and (2) to investigate the relation between transport activity and the expression level of PEPT1. Based on the findings of uptake studies and the quantification of PEPT1 mRNA, we defined the amount of PEPT1 mRNA as an index for the expression level of PEPT1, and we described mathematically the maximal velocity (V_{max}) of PEPT1. Furthermore, using two clones differing in the expression level of PEPT1, validation of the improved model of Gly-Sar transport was performed.

Materials and methods

Materials

[^{14}C]Gly-Sar (4.07 GBq/mmol) was obtained from Moravek Biochemicals, Inc. (Brea, CA, USA) and D-[1-^{3}H(N)] mannitol (629 GBq/mmol) was from NEN Life Science Products, Inc. (Boston, MA, USA). Gly-Sar was purchased from Sigma Chemical Co. (St. Louis, MO, USA). All other chemicals used were of the highest purity available.

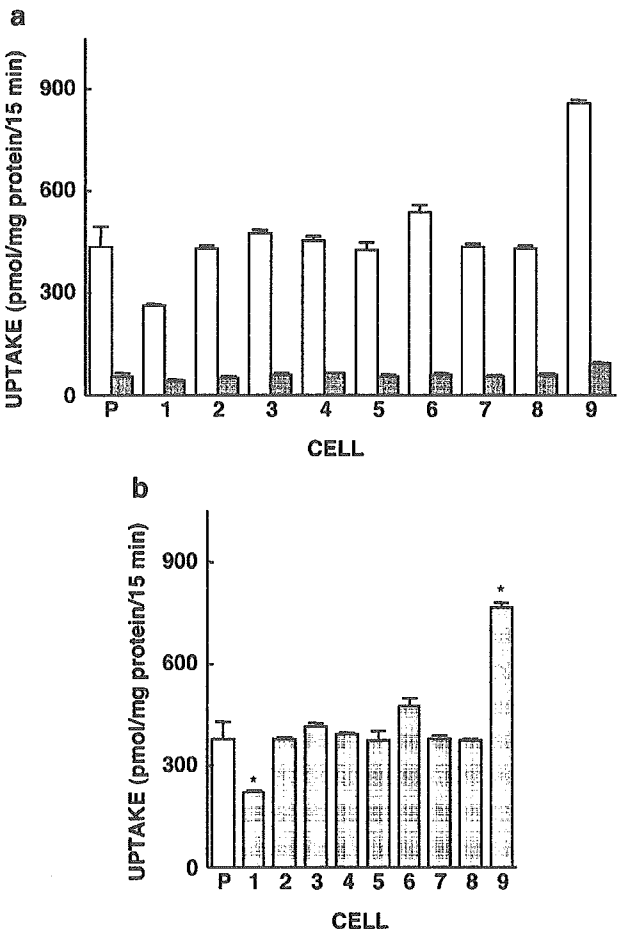

Fig. 1 [^{14}C]Gly-Sar uptake from the apical side in the parental Caco-2 cells (*P*) and in the nine cell lines (*clones 1–9*) cloned from Caco-2 cells. **a** The cell monolayers were incubated at 37°C for 15 min with an incubation medium containing 20 μM [^{14}C]Gly-Sar (pH 6.0) in the absence (*open column*) or in the presence (*hatched column*) of 10 mM unlabeled Gly-Sar. After washing, the radioactivity of dissolved cells was measured. **b** The specific uptake of PEPT1 was calculated by subtracting the uptake in the presence of 10 mM Gly-Sar from that in its absence. Each column represents the mean ± SE of six independent monolayers from two separate experiments. *P<0.05, significantly different from the parental Caco-2 cells

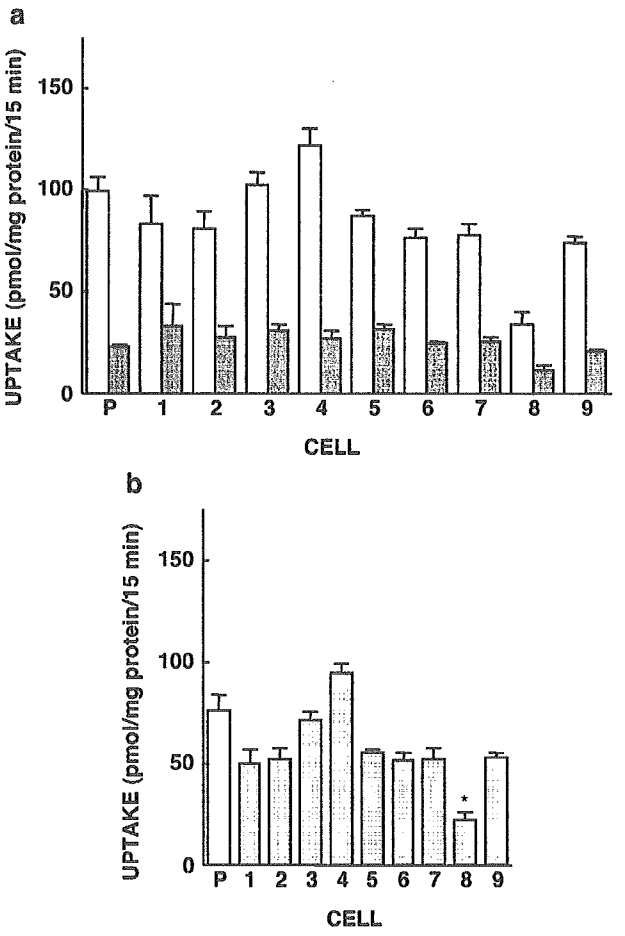

Fig. 2 [^{14}C]Gly-Sar uptake from the basolateral side in the parental Caco-2 cells (*P*) and in the nine cell lines (*clones 1–9*) cloned from Caco-2 cells. **a** The cell monolayers were incubated at 37°C for 15 min with the incubation medium containing 20 μM [^{14}C]Gly-Sar (pH 6.0) in the absence (*open column*) or in the presence (*hatched column*) of 10 mM unlabeled Gly-Sar. After washing, the radioactivity of dissolved cells was measured. **b** The specific uptake of PEPT1 was calculated by subtracting the uptake in the presence of 10 mM Gly-Sar from that in its absence. Each column represents the mean ± SE of six independent monolayers from two separate experiments. *P<0.05, significantly different from the parental Caco-2 cells

Cell culture and recloning of Caco-2 cells

Caco-2 cells at passage 18, obtained from the American Type Culture Collection (ATCC HTB37), were maintained by serial passage in plastic culture dishes, as described previously [12]. To measure the uptake of [^{14}C]Gly-Sar from the apical or basolateral side, Caco-2 cells were seeded on 12-well cluster plates (1×10^4 cells/well, 1 ml of culture medium) or on microporous membrane filters (3.0-μm pores, 1 cm^2) inside Transwell cell culture chambers (Costar, Cambridge, MA, USA) at a cell density of 6.6×10^4 cells/filter, respectively. Each Transwell chamber was filled with 0.33 and 1 ml of culture medium in the apical and basolateral compartments, respectively. For transepithelial transport studies, Caco-2 cells were seeded on microporous membrane filters (3.0-μm pores, 4.7 cm^2) at a density of 3×10^5 cells/filter and cultured with 1.5 and 2.6 ml of culture medium on the apical and basolateral sides, respectively. To prepare total RNA from the cells, Caco-2 cells were seeded on 35-mm plastic dishes (2×10^4 cells/dish, 2 ml of culture medium). Cell monolayers were given a fresh culture medium every 2–4 days and were used on the 14th or 15th day for experiments.

To obtain cell lines with different expression levels of PEPT1, parental Caco-2 cells at passage 38 were seeded on 100-mm plastic dishes at a density of 1×10^2 cells/dish. Between 3 and 4 weeks, single colonies appeared and nine colonies were picked up for subsequent experiments. In the present study, parental and cloned Caco-2 cells were used between passages 41 and 48.

Uptake and transport studies with cell monolayers

The uptake of [^{14}C]Gly-Sar from the apical or basolateral side was determined and transport studies were performed as described previously [21, 24]. Briefly, Caco-2 cells were preincubated with 2 ml of the incubation medium (pH 7.4) on both the apical and the basolateral sides for 10 min, and then 2 ml of 20 μM [^{14}C]Gly-Sar, including 0.5 μCi/ml [^{3}H]mannitol (pH 6.0) or the incubation medium (pH 7.4), was added to the apical or basolateral side, respectively. After incubation for the indicated period at 37°C, accumulation and transepithelial transport of [^{14}C]Gly-Sar and [^{3}H]mannitol were determined by liquid scintillation counting.

Quantification of PEPT1 mRNA expression

The expression levels of PEPT1 mRNA were determined by real-time polymerase chain reaction (PCR), as described previously [16]. Briefly, aliquots of 0.5 μg of total RNA, isolated from original Caco-2 cells and from each clone using the RNeasy Mini Kit (Qiagen, Hilden, Germany), were reverse-transcribed in 20 μl of reaction mixture. Real-time PCR was performed in a total volume of 20 μl containing 0.05 μg of cDNA, 1 μM forward and reverse primers, 0.2 μM TaqMan probe, and 10 μl of TaqMan Universal PCR Master Mix (Applied Biosystems, Foster City, CA, USA) under the following conditions: 50 cycles of 94°C for 15 s and 60°C for 60 s. The primer/probe set for the specific amplification of PEPT1 (accession no. NM_005703) was designed according to parameters incorporated in the Primer Express software (PE Biosystems, Foster City, CA, USA). The forward and reverse primers were ATTGTGTCGCTCTCCATTGTCTAC (positions 306–329) and ATGACCTCACAGACCACAACCAT (positions 389–367), respectively. The sequence of TaqMan probe was TTGGACAAGCAGTCACCTCAGTAAGCT CCA, corresponding to positions 334–363.

Data analysis

Each experimental point represents the mean ± SE of three to nine measurements from one to three separate experiments. Data from uptake studies were analyzed statistically by one-way analysis of variance followed by Sheffé's test. Kinetic parameters of isolated clones were statistically compared with those of parental cells by nonpaired *t* test.

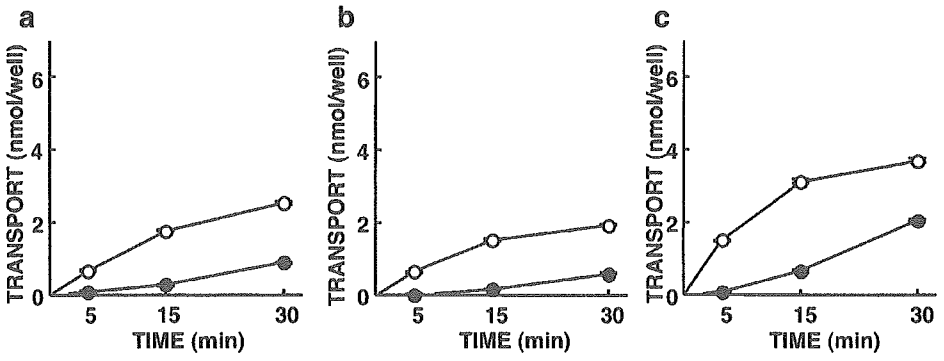

Fig. 3 [^{14}C]Gly-Sar transport from the apical side in the parental Caco-2 cells (**a**), in clone 1 (**b**), and in clone 9 (**c**). After preincubation, the cell monolayers were incubated at 37°C with 20 μM [^{14}C]Gly-Sar (pH 6.0) containing [^{3}H]mannitol, and the incubation medium (pH 7.4) was added to the apical and basolateral sides, respectively. At the indicated time, the accumulation (*circle*) and the transepithelial transport (*filled circle*) of [^{14}C]Gly-Sar were determined. The radioactivity of [^{3}H]mannitol was measured simultaneously for validation of paracellular flux (not shown). Each *symbol* represents the mean ± SE of three independent monolayers. When *error bars* are not shown, they are smaller than the *symbols*

Results

[^{14}C]Gly-Sar uptake from apical and basolateral sides in parental Caco-2 cells and in nine clones obtained by recloning of Caco-2 cells

It has been reported that Caco-2 cells, which are a useful model of intestinal epithelial cells, are heterogeneous [28]. Therefore, recloning of the parental Caco-2 cells was performed to obtain a series of cell lines differing in the expression level of PEPT1; nine clones were isolated. Compared with the parental Caco-2 cells, [^{14}C]Gly-Sar uptake from the apical side in clone 1 was markedly lower, whereas that in clone 9 was about twofold (Fig. 1). The other seven clones exhibited activity for the uptake of [^{14}C]Gly-Sar comparable to that of the parental Caco-2 cells. On the other hand, [^{14}C]Gly-Sar uptake from the basolateral side in all the clones except clone 8 did not differ significantly from that in the parental Caco-2 cells: clone 8 cells exhibited less activity (Fig. 2).

Transepithelial transport of [^{14}C]Gly-Sar in parental Caco-2 cells and in clones 1 and 9

Uptake studies suggested that two clones (clones 1 and 9) may be useful for the assessment of the transepithelial transport of Gly-Sar because the expression level of PEPT1 in each clone is different from that in the parental Caco-2 cells and because the activities of the basolateral peptide transporter in these cells are comparable. We then examined Gly-Sar transport in the absorptive direction of these cells. As shown in Fig. 3, the transepithelial transport and the accumulation of [^{14}C]Gly-Sar in clones 1 and 9 were less and greater than those in the Caco-2 cells, respectively. On the other hand, permeation of [^{3}H]mannitol, which is an index of paracellular flux, did not differ in these cells (data not shown). Results demonstrated that the intensity of PEPT1 activity obviously affects not only the accumulation but also the transepithelial transport of substrates.

Table 1 Michaelis–Menten constant (K_m) and the maximal velocity (V_{max}) of [^{14}C]Gly-Sar uptake by PEPT1 in the parental Caco-2 cells, in clone 1, and in clone 9

Cell line	Kinetic parameters	
	K_m (mM)	V_{max} (nmol/mg protein per 15 min)
Parental Caco-2	1.04±0.08	14.2±0.23
Clone 1	0.93±0.15	10.3±0.43*
Clone 9	0.98±0.11	33.0±2.64*

[^{14}C]Gly-Sar uptake from the apical side in each cell line was measured at various concentrations for 15 min, and then the kinetic parameters were determined by nonlinear least squares regression analysis according to the Michaelis–Menten equation. Each value represents the mean ± SE of three independent experiments
*P<0.05, significantly different from the value of the parental cells

Kinetic analysis of [^{14}C]Gly-Sar uptake by PEPT1

Next, we performed a kinetic analysis of [^{14}C]Gly-Sar uptake from the apical side in the parental cells and in clones 1 and 9. As illustrated in Fig. 4, [^{14}C]Gly-Sar uptake in these cells was saturable, and kinetic parameters were estimated according to the Michaelis–Menten equation using nonlinear least squares regression analysis. As summarized in Table 1, the maximal velocity (V_{max}) of [^{14}C]Gly-Sar uptake in clones 1 and 9 was significantly lower and greater than that in the parental Caco-2 cells, respectively. However, Michaelis–Menten constants (K_m) were comparable among these cells. These findings suggested that the differences in the activities of [^{14}C]Gly-Sar uptake among the three cell lines are caused by the different expression levels of PEPT1 protein.

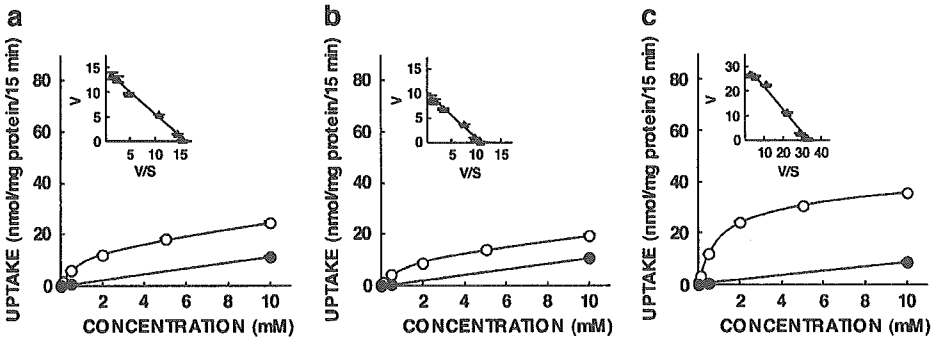

Fig. 4 Concentration dependence of [^{14}C]Gly-Sar uptake from the apical side in the parental Caco-2 cells (**a**), in clone 1 (**b**), and in clone 9 (**c**). [^{14}C]Gly-Sar uptake was measured at various concentrations for 15 min in the absence (*circle*) or in the presence (*filled circle*) of 50 mM glycyl-leucine. These figures show the representative data of three experiments. Each *point* represents the mean ± SE of three monolayers. When *error bars* are not shown, they are smaller than the *symbols*. *Insets*: Eadie–Hofstee plots of [^{14}C]Gly-Sar uptake after correction for nonspecific component (*filled triangle*). *V* Uptake rate (nmol/mg protein per 15 min), *S* [^{14}C]Gly-Sar concentration (mM)

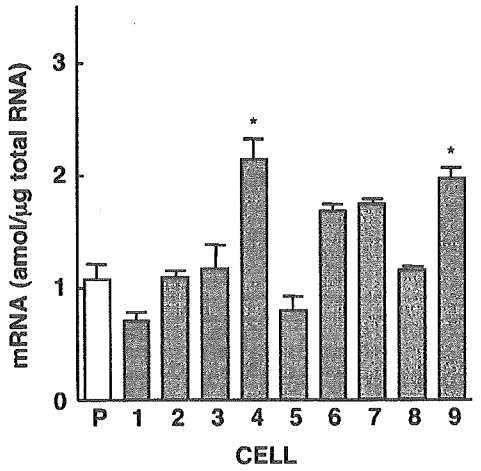

Fig. 5 Quantification of PEPT1 mRNA expressed in the parental Caco-2 cells (*P*) and in the nine cell lines (*clones1–9*). Total cellular RNA was extracted from the cells and then reverse-transcribed. The mRNA levels of PEPT1 in these cells were determined by real-time PCR using an ABI Prism 7700 sequence detector. Each column represents the mean ± SE of five to eight independent monolayers from two or three separate experiments. **P*<0.05, significantly different from the parental Caco-2 cells

Expression levels of PEPT1 mRNA in parental Caco-2 cells and in isolated clones

Moreover, the amount of PEPT1 mRNA expressed in the parental Caco-2 cells and in the nine clones was determined by real-time PCR. As shown in Fig. 5, the expression level of PEPT1 mRNA in clone 1 was lower than that in the parental cells. In contrast, clone 9 displayed a level of expression that was higher than that of the parental Caco-2 cells. These findings were consistent with the activity of [^{14}C]Gly-Sar uptake from the apical side in these cells (Fig. 1). On the other hand, clone 4 exhibited a greater level of PEPT1 mRNA expression, despite activities of PEPT1 comparable to those of the parental Caco-2 cells.

To further examine whether the expression level of PEPT1 mRNA can serve as an indicator of PEPT1 activity, the correlation between the uptake of [^{14}C]Gly-Sar and the amount of PEPT1 mRNA was investigated in the parental and cloned cells at passages 41 and 46 in order to increase the number of samples. Figure 6 shows the linear regression of the activity of [^{14}C]Gly-Sar uptake from the apical side against the expression level of PEPT1 mRNA in the parental Caco-2 cells and in the nine clones. A positive linear correlation was observed with r=0.55.

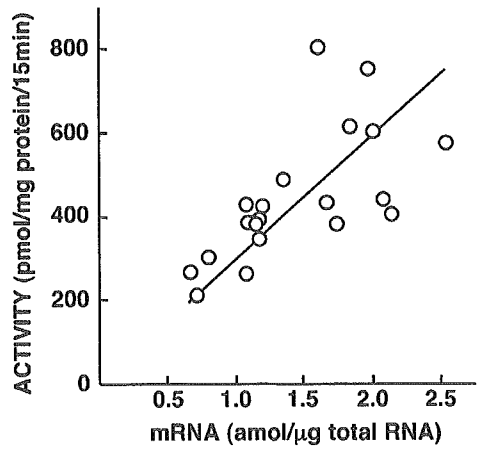

Fig. 6 The linear regression of the activity of [^{14}C]Gly-Sar uptake against the expression level of PEPT1 mRNA in the parental Caco-2 cells and in the nine clones. [^{14}C]Gly-Sar uptake was measured experimentally, and the amount of PEPT1 mRNA was determined by real-time PCR in the same batch of the respective cells. Each *symbol* was plotted using the mean of [^{14}C]Gly-Sar uptake and that of mRNA expression in three independent monolayers

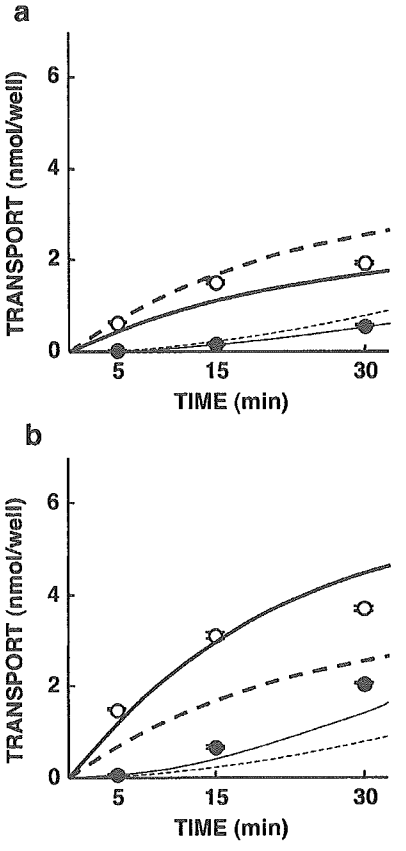

Fig. 7 Simulation of Gly-Sar transport in two clones. The accumulation and the transepithelial transport of 20 μM Gly-Sar in clone 1 (**a**) and in clone 9 (**b**) in the absorptive direction were simulated using the expanded computational model. The curves were delineated using the values of Gly-Sar transport calculated every 0.01 min with a program written in Visual Basic.NET. Numeric integration is based on Euler's method. The *bold* and *fine curves* represent the simulated accumulation and the transepithelial transport of Gly-Sar, respectively. The *solid* and *broken curves* display the simulation by the expanded and the previous models for Gly-Sar transport, respectively. The *symbols* represent the experimental data of the accumulation (*circle*) and the transepithelial transport (*filled circle*) of [^{14}C]Gly-Sar

Simulation for transepithelial transport of Gly-Sar

Based on the above findings, we chose the amount of PEPT1 mRNA as an index for the intensity of the transport activity of PEPT1. In the previous model, the maximal velocity (V_{max}) of PEPT1 in the influx direction was estimated using the parental Caco-2 cells and was defined as a constant value [11]. To incorporate mathematically the amount of PEPT1 mRNA to the simulator as a relative factor of PEPT1 activity, the V_{max} of PEPT1 in the influx direction was regarded as a variable using the following equation: $V_{max\,PEPT1,\,uptake} = 4.164 \times mRNA/1.073$ where "4.164" is the V_{max} value (nmol/min per milligram of protein) determined in the previous study [11] and "1.073" is the mean of PEPT1 mRNA (amol/μg total RNA) expressed in the parental Caco-2 cells in this study. $V_{maxPEPT1,\,uptake}$ represents the V_{max} value after correction (nmol/min per milligram of protein), and mRNA stands for the amount of mRNA (amol/μg total RNA) in the cells compared.

To validate the model, Gly-Sar transport in clones 1 and 9 was simulated using both the previous model and the improved model. The mean of the amount of PEPT1 mRNA expressed in clones 1 and 9 was 0.712 and 1.963 (amol/μg total RNA), respectively. As shown in Fig. 7, the simulation using the model developed in this study corresponded more closely with experimental data than that using the previous model, indicating that the improved model can achieve a change in the expression level of PEPT1.

Discussion

It has been proposed that computational modeling can provide a tool for the reproduction and understanding of physiological and molecular biological phenomena in which multiple factors participate [5, 9, 15, 22]. Because of the diversity and multispecificity of drug transporters, the behavior of a drug is complicated; therefore, computational modeling of drug transporters will be useful in predicting drug behavior and in studying the relationship and contribution of transporters.

Recently, based on a detailed examination of the functional properties of PEPT1 and the basolateral peptide transporter, we constructed a mathematical model of Gly-Sar transport in Caco-2 cells [11]. This model could predict Gly-Sar transport, but could not achieve a change in the expression level of PEPT1. With respect to various drug transporters including PEPT1, the expression levels of transporters were proven to affect the pharmacokinetic properties of substrates [8, 18, 20]. Furthermore, it has been demonstrated that the expression levels of PEPT1 in the small intestine differ among the segments [17] and that PEPT1 is regulated by a variety of factors [2]. Therefore, to establish a simulator of drug absorption, it is essential that the model encompasses an alteration in PEPT1 expression. To address this issue, the V_{max} value of PEPT1 is defined as a variable reflecting the expression level and is described mathematically using the amount of PEPT1 mRNA in this study. With this improved model, Gly-Sar transport in cloned cells expressing the lowest and the highest levels of PEPT1 was predicted more accurately than with the previous model (Fig. 7), indicating that our model can simulate the behavior of Gly-Sar in Caco-2 cells even if the expression level of PEPT1 is altered.

Chu et al. [4] demonstrated that PEPT1 protein expression and cephalexin uptake exhibited a good correlation using Caco-2 cells expressing PEPT1 at various levels. Furthermore, they also found that PEPT1 protein expression was well-correlated with PEPT1 mRNA level, although the data were not shown. Consistent with their report, a correlation between the transport activity and the mRNA expression of PEPT1 was confirmed in cells isolated from the parental Caco-2 cells in this study. These results suggest that the amount of PEPT1 mRNA is an appropriate index for a mathematical description of the PEPT1 expression level when a change in the activity of PEPT1 accompanies that in the PEPT1 gene expression. Besides transcriptional regulation, it has been reported that several signals, such as insulin [25] and leptin [3], induce an alteration in the PEPT1 protein expression without any change in the amount of PEPT1 mRNA. The mechanism of insulin and leptin regulation was suggested to be increased trafficking of the PEPT1 proteins from the cytoplasmic pool to the apical membranes. Because of inconvenience and difficulty, however, the determination of absolute PEPT1 protein expression level seems to be unavailable as an index of PEPT1 expression for improvement of the simulator. Therefore, we chose the expression of PEPT1 mRNA as an index and incorporated it into our model. Further studies and new technologies are needed to overcome problems in the handling of regulation that do not parallel alterations in the PEPT1 mRNA expression.

It was observed that the activity of [^{14}C]Gly-Sar uptake in clone 4 was comparable to that in the parental Caco-2 cells in spite of the higher expression of PEPT1 mRNA. In addition, more dispersion was observed in the analysis of the correlation between the activity and the mRNA expression of PEPT1 in this study compared to the previous study [4]. These differences may be caused by used cells: Chu et al. [4] used PEPT1-overexpressed Caco-2 cells established by an adenoviral transfection system, whereas we used clones isolated from the parental Caco-2 cells. It is possible that not only the expression of PEPT1 but also that of other molecules affecting the apparent activity of Gly-Sar uptake (such as Na^+/H^+ exchanger 3) [13] differ from that of the clones. Likely, several factors (other than PEPT1) among the parental cloned cells may be responsible for the slight disagreement in the simulation using the improved model with experimental data (Fig. 7). These findings suggest that, besides PEPT1, other factors should be described mathematically and incorporated into the model.

In conclusion, to adjust the previous model for the simulation of Gly-Sar transport in accordance with a change in the expression level of PEPT1, the V_{max} value of PEPT1 in the influx direction was defined mathematically using the

amount of PEPT1 mRNA as an index of the PEPT1 expression level. The improved model could well reproduce the transport of Gly-Sar in the cells expressing PEPT1 at the highest and the lowest levels. These findings suggest that our model can predict Gly-Sar transport even when PEPT1 is expressed at a different level and that the developed model may underlie a simulator for the prediction of drug absorption in the small intestine.

Acknowledgements This work was supported, in part, by the Leading Project for Biosimulation, the 21st Century COE Program "Knowledge Information Infrastructure for Genome Science," and a Grant-in-Aid for Scientific Research from the Ministry of Education, Culture, Sports, Science, and Technology of Japan. Megumi Irie is a Research Fellow of the Japan Society for the Promotion of Science.

References

1. Adibi SA (1997) The oligopeptide transporter (Pept-1) in human intestine: biology and function. Gastroenterology 113:332–340
2. Adibi SA (2003) Regulation of expression of the intestinal oligopeptide transporter (Pept-1) in health and disease. Am J Physiol Gastrointest Liver Physiol 285:G779–G788
3. Buyse M, Berlioz F, Guilmeau S, Tsocas A, Voisin T, Péranzi G, Merlin D, Laburthe M, Lewin MJM, Rozé C, Bado A (2001) PepT1-mediated epithelial transport of dipeptides and cephalexin enhanced by luminal leptin in the small intestine. J Clin Invest 108:1483–1494
4. Chu X-Y, Sánchez-Castaño GP, Higaki K, Oh D-M, Hsu C-P, Amidon GL (2001) Correlation between epithelial cell permeability of cephalexin and expression of intestinal oligopeptide transporter. J Pharmacol Exp Ther 299:575–582
5. Clancy CE, Rudy Y (1999) Linking a genetic defect to its cellular phenotype in a cardiac arrhythmia. Nature 400:566–569
6. Daniel H (2004) Molecular and integrative physiology of intestinal peptide transport. Annu Rev Physiol 66:361–384
7. Daniel H, Kottra G (2004) The proton oligopeptide cotransporter family SLC15 in physiology and pharmacology. Pflugers Arch 447:610–618
8. Hashida T, Masuda S, Uemoto S, Saito H, Tanaka K, Inui K (2002) Pharmacokinetic and prognostic significance of intestinal MDR1 expression in recipients of liver-donor liver transplantation. Clin Pharmacol Ther 69:308–316
9. Hoffmann A, Levchenko A, Scott ML, Baltimore D (2002) The IκB–NF-κB signaling module: temporal control and selective gene activation. Science 298:1241–1245
10. Inui K, Yamamoto M, Saito H (1992) Transepithelial transport of oral cephalosporins by monolayers of intestinal epithelial cell line Caco-2: specific transport systems in apical and basolateral membranes. J Pharmacol Exp Ther 261:195–201
11. Irie M, Terada T, Okuda M, Inui K (2004) Efflux properties of basolateral peptide transporter in human intestinal cell line Caco-2. Pflugers Arch 449:186–194
12. Irie M, Terada T, Sawada K, Saito H, Inui K (2001) Recognition and transport characteristics of nonpeptidic compounds by basolateral peptide transporter in Caco-2 cells. J Pharmacol Exp Ther 298:711–717
13. Kennedy DJ, Leibach FH, Ganapathy V, Thwaites DT (2002) Optimal absorptive transport of the dipeptide glycylsarcosine is dependent on functional Na^+/H^+ exchange activity. Pflugers Arch 445:139–146
14. Leibach FH, Ganapathy V (1996) Peptide transporters in the intestine and the kidney. Annu Rev Nutr 16:99–119
15. Matsuoka S, Sarai N, Kuratomi S, Ono K, Noma A (2003) Role of individual ionic current systems in ventricular cells hypothesized by a model study. Jpn J Physiol 53:105–123
16. Motohashi H, Sakurai Y, Saito H, Masuda S, Urakami Y, Goto M, Fukatsu A, Ogawa O, Inui K (2002) Gene expression levels and immunolocalization of organic ion transporters in the human kidney. J Am Soc Nephrol 13:866–874
17. Naruhashi K, Sai Y, Tamai I, Suzuki N, Tsuji A (2002) Pept1 mRNA expression is induced by starvation and its level correlates with absorptive transport of cefadroxil longitudinally in the rat intestine. Pharm Res 19:1417–1423
18. Pan X, Terada T, Irie M, Saito H, Inui K (2002) Diurnal rhythm of H^+-peptide cotransporter in rat small intestine. Am J Physiol Gastrointest Liver Physiol 283:G57–G64
19. Saito H, Inui K (1993) Dipeptide transporters in apical and basolateral membranes of the human intestinal cell line Caco-2. Am J Physiol Gastrointest Liver Physiol 265:G289–G294
20. Sakurai Y, Motohashi H, Ueo H, Masuda S, Saito H, Okuda M, Mori N, Matsuura M, Doi T, Fukatsu A, Ogawa O, Inui K (2004) Expression levels of renal organic anion transporters (OATs) and their correlation with anionic drug excretion in patients with renal diseases. Pharm Res 21:61–67
21. Sawada K, Terada T, Saito H, Inui K (2001) Distinct transport characteristics of basolateral peptide transporters between MDCK and Caco-2 cells. Pflugers Arch 443:31–37
22. Schoeberl B, Eichler-Jonsson C, Gilles ED, Müller G (2002) Computational modeling of the dynamics of the MAP kinase cascade activated by surface and internalized EGF receptors. Nat Biotechnol 20:370–375
23. Terada T, Inui K (2004) Peptide transporters: structure, function, regulation and application for drug delivery. Curr Drug Metab 5:85–94
24. Terada T, Sawada K, Saito H, Inui K (1999) Functional characteristics of basolateral peptide transporter in the human intestinal cell line Caco-2. Am J Physiol Gastrointest Liver Physiol 276:G1435–G1441
25. Thamotharan M, Bawani SZ, Zhou X, Adibi SA (1999) Hormonal regulation of oligopeptide transporter Pept-1 in a human intestinal cell line. Am J Physiol Cell Physiol 276: C821–C826
26. Thwaites DT, Brown CDA, Hirst BH, Simmons NL (1993) Transepithelial glycylsarcosine transport in intestinal Caco-2 cells mediated by expression of H^+-coupled carriers at both apical and basal membranes. J Biol Chem 268:7640–7642
27. Thwaites DT, Brown CDA, Hirst BH, Simmons NL (1993) H^+-coupled dipeptide (glycylsarcosine) transport across apical and basal borders of human intestinal Caco-2 cell monolayers display distinctive characteristics. Biochim Biophys Acta 1151:237–245
28. Vachon PH, Beaulieu J-F (1992) Transient mosaic patterns of morphological and functional differentiation in the Caco-2 cell line. Gastroenterology 103:414–423
29. Yang CY, Dantzig AH, Pidgeon C (1999) Intestinal peptide transport systems and oral drug availability. Pharm Res 16:1331–1343

Pharmaceutical Research (© 2006)
DOI: 10.1007/s11095-006-9665-2

Research Paper

Androgen Receptor is Responsible for Rat Organic Cation Transporter 2 Gene Regulation but not for rOCT1 and rOCT3

Jun-ichi Asaka,[1] Tomohiro Terada,[1] Masahiro Okuda,[1] Toshiya Katsura,[1] and Ken-ichi Inui[1,2]

Received October 18, 2005; accepted December 7, 2005

Purpose. Organic cation transporters 1–3 (OCT1–3; Slc22a1–3) mediate the membrane transport of organic cations in the kidney. We previously reported that rat (r)OCT2 expression in the kidney was regulated by testosterone. In this study, we examined the transcriptional mechanisms underlying the testosterone-dependent regulation of rOCT2 expression.
Methods. Approximately 3000-bp fragments of the rOCT1–3 promoter region were isolated, and promoter activities were measured in the renal epithelial cell line LLC-PK_1 with the coexpression of rat androgen receptor.
Results. Among reporter constructs tested, only rOCT2 promoter activity was stimulated by testosterone. This stimulation was suppressed by nilutamide, an antiandrogen drug. Reporter assays using deletion constructs and mutational constructs of putative androgen response elements (ARE) in the rOCT2 promoter region suggested that two AREs, located at approximately −3000 and −1300, respectively, play an important role in the induction by testosterone.
Conclusions. Testosterone induces the expression of rOCT2, but not of rOCT1 and rOCT3, via the AR-mediated transcriptional pathway. This is the first study to address the transcriptional mechanisms of testosterone-dependent gene regulation of the Slc22 family.

KEY WORDS: gender difference; kidney; promoter; rOCT2; testosterone.

INTRODUCTION

Proximal tubules play important roles in the renal elimination of drugs. Cationic drugs are secreted from blood to urine by combined efforts of two distinct classes of organic cation transporters: one driven by the transmembrane electrical potential difference in the basolateral membranes, and the other driven by the transmembrane H^+ gradient in the brush-border membranes (1). Molecular cloning studies identified three kinds of organic cation transporters (OCT1–3), and their physiological and pharmacokinetic roles have been evaluated (2,3). Rat (r)OCT1 (Slc22a1) is expressed abundantly in the liver and kidney (4), whereas rOCT2 (Slc22a2) is expressed in the kidney, but not in the liver (5). These transporters are localized to the basolateral membranes of renal proximal tubules (6,7). rOCT3 (Slc22a3) is expressed predominantly in the placenta, and also in the intestine, heart, brain, lung, and very weakly in the kidney (8). Functional studies using heterologous expression systems revealed that all OCTs recognized a variety of organic cations with different molecular structures including tetraethylammonium, 1-methyl-4-phenylpyridinium, N^1-methylnicotinamide, choline, and dopamine (8,9).

It was reported that the uptake of tetraethylammonium was greater in renal cortical slices of male rats than female rats (10), suggesting gender differences in the basolateral membrane transport activity for organic cations. We found that expression level of rOCT2, but neither rOCT1 nor rOCT3, in the kidney was much higher in males than females and suggested that rOCT2 is responsible for gender differences in renal basolateral membrane organic cation transport activity (11). Furthermore, we demonstrated that treatment of male and female rats with testosterone significantly increased rOCT2 expression in the kidney (12). These results suggested that testosterone plays a pivotal role in the transcriptional regulation of the rOCT2 gene. However, no information has been available to demonstrate this process.

Androgens, such as testosterone, are main hormones responsible for the male phenotype (13). As with other steroid hormones, many effects of androgen are mediated by a specific intracellular androgen receptor (AR; NR3C4). AR activated by testosterone binds to the androgen response element (ARE) in the 5′-flanking region of target genes and is responsible for the expression of various genes such as the C3 subunit of prostatin (14) and prostate-specific antigen gene (15). Based on our previous studies, we hypothesized that AR could be involved in the regulation of the rOCT2 gene.

[1] Department of Pharmacy, Kyoto University Hospital, Faculty of Medicine, Kyoto University, Sakyo-ku, Kyoto 606-8507, Japan.
[2] To whom correspondence should be addressed. (e-mail: inui@kuhp.kyoto-u.ac.jp)

ABBREVIATIONS: AR, androgen receptor; ARE, androgen response element; bp, base pair; CYP, cytochrome P450; DMEM, Dulbecco's modified Eagle's medium; FBS, fetal bovine serum; MMTV, mouse mammary tumor virus; OCT, organic cation transporter; PCR, polymerase chain reaction; RACE, rapid amplification of cDNA ends.